Article

Light-driven anaerobic microbial oxidation of manganese

https://doi.org/10.1038/s41586-019-1804-0

Received: 8 June 2018

Accepted: 8 October 2019

Published online: 4 December 2019

Mirna Daye[1]*, Vanja Klepac-Ceraj[2], Mihkel Pajusalu[1], Sophie Rowland[2], Anna Farrell-Sherman[2], Nicolas Beukes[3], Nobumichi Tamura[4], Gregory Fournier[1] & Tanja Bosak[1]*

Oxygenic photosynthesis supplies organic carbon to the modern biosphere, but it is uncertain when this metabolism originated. It has previously been proposed[1,2] that photosynthetic reaction centres capable of splitting water arose by about 3 billion years ago on the basis of the inferred presence of manganese oxides in Archaean sedimentary rocks. However, this assumes that manganese oxides can be produced only in the presence of molecular oxygen[3], reactive oxygen species[4,5] or by high-potential photosynthetic reaction centres[6,7]. Here we show that communities of anoxygenic photosynthetic microorganisms biomineralize manganese oxides in the absence of molecular oxygen and high-potential photosynthetic reaction centres. Microbial oxidation of Mn(II) under strictly anaerobic conditions during the Archaean eon would have produced geochemical signals identical to those used to date the evolution of oxygenic photosynthesis before the Great Oxidation Event[1,2]. This light-dependent process may also produce manganese oxides in the photic zones of modern anoxic water bodies and sediments.

Manganese and more than 30 of its described oxides and hydroxides mediate the cycling of various trace metals and nutrients in the environment. The ability of microorganisms to oxidize Mn(II) anaerobically has also been hypothesized to have been a critical step in the evolution of oxygenic photosynthesis on the early Earth[6]. However, modern microorganisms are not known to anaerobically oxidize manganese. Here we demonstrate this activity in active microbial cultures that grow in the presence of nanomolar concentrations of oxygen, relevant for the Archaean Earth.

Inoculum for the enrichment cultures of strictly anaerobic, photosynthetic biofilms came from the meromictic Fayetteville Green Lake (New York, USA). The most abundant phototroph in the sulfidic photic zone of this lake is the green sulfur bacterium *Chlorobium* sp.[8], a microorganism that uses sulfide as the electron donor for photosynthesis. Biofilms (Fig. 1a) containing *Chlorobium* sp. and other strict anaerobic microorganisms were enriched in a minimal medium amended with 20–50 μM Na_2S and 1 mM $MnCl_2$ and equilibrated with an anaerobic atmosphere of 80% N_2 and 20% CO_2 at pH 7. The concentration of O_2 in the medium was lower than 2 nM during the entire experiment, both in the presence and the absence of cells (Extended Data Fig. 1, Methods). These experimental concentrations match the upper estimates for the Archaean Earth[9]. The anaerobic medium also lacked other potential oxidants for Mn(II), such as nitrite, nitrate and H_2O_2, and these species were not produced in sterile controls ('Concentrations of dissolved species in culture media' in the Methods).

Four times more biomass grew in photosynthesizing cultures relative to the cultures incubated in the dark ($P << 0.001$) (Fig. 1b). The enrichment protocol yielded a stable community that contained *Chlorobium*, *Paludibacter*, *Acholeplasma*, *Geobacter*, *Desulfomicrobium*, *Clostridium*, *Acetobacterium* and several other bacteria (Fig. 1c). The *Chlorobium* sp. was the most abundant taxon across all conditions, as well as the only identifiable phototroph (Fig. 1c). Its genome was 98.4% similar to *Chlorobium limicola* Frassasi.

This microbial community was essential for the precipitation of minerals and oxidation of manganese. Manganese-rich dolomite was the most abundant precipitate in photosynthetic cultures amended with 0.1–1 mM Mn(II) and 20–250 μM sulfide[10] (Fig. 2, Extended Data Fig. 2a, b, d), which is comparable to the estimated dissolved Mn(II) concentrations (0.1 mM) maintained by the precipitation of manganese-containing carbonate minerals on Archaean carbonate platforms[11,12]. Cultures incubated in this range of chemical conditions also contained manganese oxide minerals (Figs. 1d, 2), but cultures incubated with approximately 1 μM Mn(II) or 1 mM sulfide did not (Extended Data Fig. 2c). Precipitates were entirely absent from sterile controls incubated in the light, whereas minor calcite, less dolomite and no manganese oxides were detected in cultures shielded from the light (Fig. 2). Elemental sulfur (S^0) accumulated in cultures that did not contain oxidized manganese minerals (Extended Data Fig. 3c), as expected during the growth of *Chlorobium* sp. under conditions in which sulfide was the main photosynthetic electron donor. Abiotic reactions did not contribute detectable amounts of manganese oxides or other minerals under our experimental conditions. Instead, the microbial presence and photosynthetic activity strongly controlled the nucleation and precipitation of minerals, including manganese oxides.

To characterize the redox cycling of manganese, we examined its oxidation state by surface-sensitive methods (Extended Data Fig. 3). After two weeks, sterile controls and cultures that were incubated in the dark contained only Mn(II) (Extended Data Fig. 3a). Dolomite that formed

[1]Department of Earth, Atmospheric, and Planetary Sciences, Massachusetts Institute of Technology, Cambridge, MA, USA. [2]Department of Biological Sciences, Wellesley College, Wellesley, MA, USA. [3]DST-NRF CIMERA, Geology Department, University of Johannesburg, Johannesburg, South Africa. [4]Advanced Light Source, Lawrence Berkeley National Laboratory, Berkeley, CA, USA. *e-mail: mirnadaye@gmail.com; tbosak@mit.edu

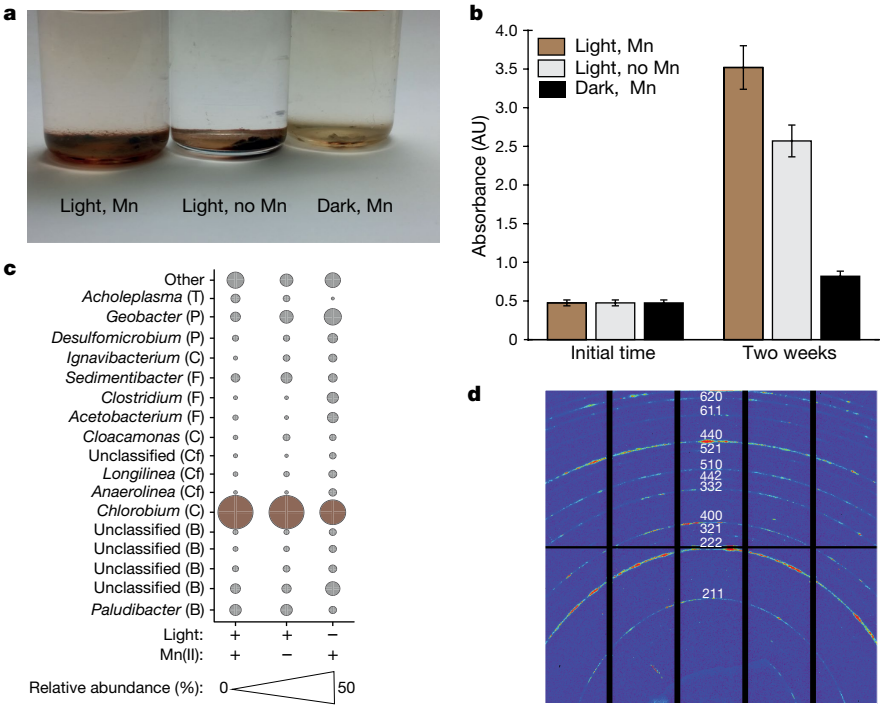

Fig. 1 | Biofilms incubated for two weeks. a, Dark brown biofilm incubated in the light with Mn(II) (left), less-extensive biofilm incubated in the light without Mn(II) (middle) and a yellow biofilm incubated in the dark with Mn(II) (right). **b**, Biomass of biofilms measured by the crystal violet assay. All incubations were performed in triplicate. AU, arbitrary units. $n = 3$ measurements; error bars ± 0.3 s.d. **c**, Microbial diversity in biofilms obtained by high-throughput Illumina sequencing of 16S rRNA genes. The most abundant taxon across all conditions was a *Chlorobium* sp. (30–60%). This microorganism was more abundant in photosynthesizing cultures. B, Bacteroidetes; C, Chlorobi; Cf, Chloroflexi; F, Firmicutes; P, Proteobacteria; T, Tenericutes. **d**, Diffraction pattern indices for Mn_3O_4 in the spectrum acquired by synchrotron micro-focused X-ray diffraction (μXRD) of a biofilm incubated in the light for two weeks.

in photosynthetic cultures contained Mn(II)[10], but we also detected Mn(II), Mn(III) and Mn(IV) in calcium manganese oxides, Mn_3O_4 and other minerals (Figs. 1d, 2, 3, Extended Data Fig. 3). The presence of manganese oxides in sulfidic photosynthetic cultures was surprising, but they were repeatedly found in biofilms that were between two weeks and two months old (Fig. 2). A colorimetric assay quantified 5.1 ± 0.8 μM of oxidized manganese in one-week-old biofilms, 7.2 ± 0.8 μM oxidizing equivalents in two-week-old biofilms and >10 μM in three-week

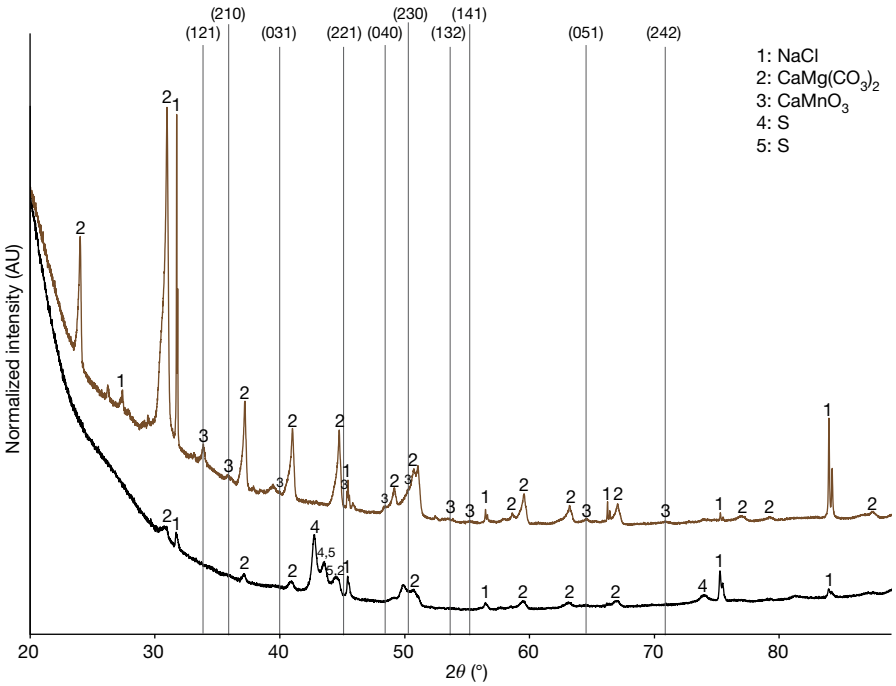

Fig. 2 | XRD spectra of biofilms incubated for two weeks. Top spectrum, biofilms incubated in the light with 1 mM Mn(II). Black lines indicate Miller indices (*hkl*) assigned to each peak of $CaMnO_3$. Bottom spectrum, biofilms incubated in the dark with 1 mM Mn(II). The sulfur phases (S) formed during the treatment to remove oxidized manganese minerals before inoculation ('Modified FGL medium' and 'Interpretation of XRD peaks' in the Methods). All data are representative of two independent experiments.

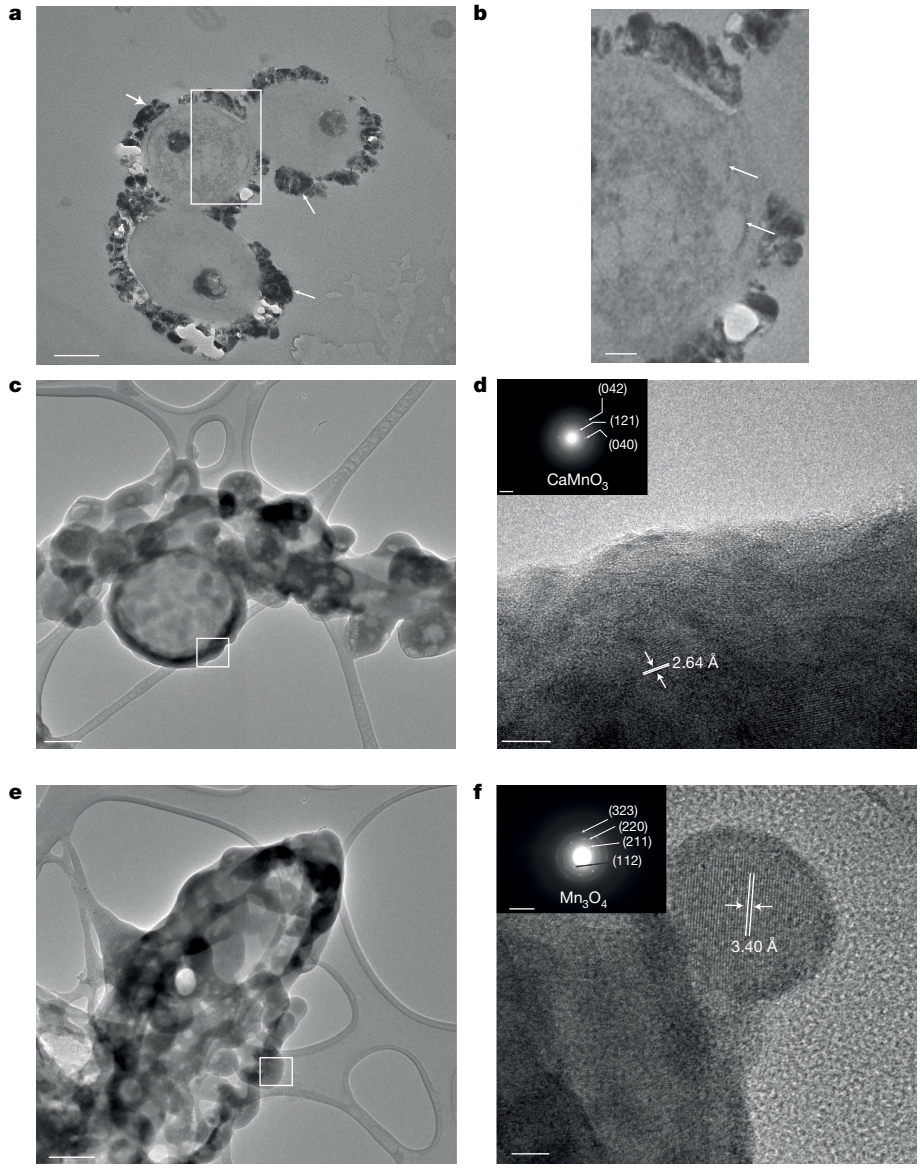

Fig. 3 | Interactions between minerals and microorganisms in biofilms incubated with Mn(II) in the light for two weeks. a, Mineral-encrusted cells (white arrows) in fixed and stained samples (transmission electron microscopy (TEM) at 80 kV); the white square indicates the area magnified in **b**. Scale bar, 200 nm. **b**, Chlorosomes (white arrows) in a cell encrusted by manganese oxide precipitates (TEM at 80 kV, fixed and stained sample). Scale bar, 50 nm. **c**, TEM at 200 kV of unprocessed and unstained mineral-encrusted microbial cells. White square indicates the region selected for selected area electron diffraction (SAED), shown in **d**. Scale bar, 200 nm. **d**, High-resolution TEM and SAED of minerals around an unstained cell from a fresh suspension of the microbial culture on a TEM grid show $CaMnO_3$ with a *d*-spacing of 2.64 Å. Scale bars, 5 nm (**d**), 5 1/nm (inset). **e**, TEM at 200 kV of unprocessed and unstained encrusted microbial cells. White square indicates the region selected for SAED shown in **f**. Scale bar, 200 nm. **f**, High-resolution TEM and SAED of minerals in the area outlined by the white square in **e** show Mn_3O_4 with a *d*-spacing of 3.40 Å. Scale bars, 5 nm (**f**), 10 1/nm (inset). All data are representative of two independent experiments.

old biofilms ('Quantification of biofilms and oxidized manganese in biofilms' in the Methods). All oxidized manganese was determined as $KMnO_4$ equivalents and none was detected in dark controls.

Oxidized manganese was present in minerals that were only found on cell surfaces (Fig. 3a) or around extracellular vesicles. These cells could be identified as *Chlorobium* sp. on the basis of the presence of large intracellular complexes of photosynthetic antennae called chlorosomes (Fig. 3b) and surface protrusions called spinae[13]. High-resolution transmission electron micrographs of fresh cell suspensions showed manganese–calcium minerals with a uniform lattice fringe that corresponded to the (121) plane with interplanar spacing of 2.64 Å of calcium manganese oxide (Fig. 3d), Mn_3O_4 (Fig. 3f) and other manganese minerals (Extended Data Fig. 2). Extracellular vesicles, spinae and manganese oxide minerals were absent from *Chlorobium* sp. when the cultures were incubated with Mn(II) in the dark or photosynthetically with 1 mM sulfide.

Light-driven manganese oxidation occurred only when *Chlorobium* sp. and other microorganisms, including *Geobacter* sp., were growing together. Oxidized manganese was present in enrichment cultures of microorganisms from Fayetteville Green Lake that contained *Chlorobium* sp., *Geobacter* sp., *Acholeplasma equifetale*, *Alistipes* sp. HGB5 and *Caldicoprobacter oshimai*, but absent from co-cultures of *Chlorobium* sp. and *Desulfomicrobium* sp. (Extended Data Fig. 4) and pure cultures of *C. limicola*. Manganese oxidizing activity was also detected in the co-cultures containing *C. limicola*, *Chlorobaculum tepidum* and *Geobacter lovleyi* (DSM 245, DSM 12025 and DSM 17278, DSMZ) ('Probing

the redox state of manganese in co-cultures' and 'Interpretation of XPS spectra' in the Methods) and the co-cultures of *C. limicola* and *G. lovleyi* (Extended Data Fig. 5). This suggests that the activity may depend on extracellular electron transfer between the latter two organisms[14] by a currently unknown mechanism. The only photosynthetic reaction centre that the genome of *Chlorobium* sp. encodes is a well-studied centre with a midpoint potential around +250 mV[15] and that cannot directly oxidize Mn(II) bicarbonate (E_h = 520–670 mV)[6,16]. *Chlorobium* sp. also lacks clear homologues of proteins that are known to oxidize manganese under aerobic conditions[17–19]. Manganese oxidation in *C. limicola* may occur by an endergonic mechanism, analogous to that proposed for the oxidation of nitrite by the *Thiocapsa* sp. strain KS1[20]. The electron transfer between *C. limicola* and *G. lovleyi* may involve high-potential cytochrome *c* in *Chlorobium* sp. and OmpB operating in reverse in *Geobacter* sp., but the Mn(II) oxidation mechanisms and potential oxidants in the co-cultures of *C. limicola* and *G. lovleyi* remain to be characterized.

The abundance of oxidized manganese in microbial biofilms, and its absence from the sterile controls, shows that microbial consortia can mediate the precipitation of manganese oxide minerals under conditions similar to those in the Archaean eon. These findings expand the diversity of minerals and redox processes beyond what was thought possible in strictly anaerobic environments or in the presence of high-potential photosynthetic reaction centres. Microbial interactions that mediate the light-dependent redox cycling of manganese and couple it to other elemental cycles remain to be identified, but can be expected in modern environments in which light, sulfide and dissolved Mn(II) coexist and sulfide concentrations do not exceed about 0.2 mM (Extended Data Table 1). The light-dependent microbial production of manganese oxides is likely to stimulate the redox cycles of carbon, sulfur, nitrogen and iron, increase the diversity of anaerobic redox transformations (including nitrification–denitrification[21]) and influence interpretations of isotopic and chemical signatures of these processes in modern anaerobic settings.

The biological production of manganese oxides under Archaean-like chemical conditions has additional major implications for determining the timing of the origin of oxygenic photosynthesis, which is currently debated[1,2,5,7]. The evolution of oxygenic photosynthesis[1] and the presence of locally oxic areas in Archaean marine systems prior to the Great Oxidation Event (GOE)[22] are inferred from geochemical signals. However, interpretations of these signals assume the former presence of manganese oxides[1,2,23,24]. For example, manganese carbonate deposits with the negative $\delta^{13}C$ values reported in the Neoarchaean Sandur schist belt (India)[25] or Mesoarchaean Witwatersrand–Mozaan strata (South Africa)[22,23] are thought to have been produced by the microbial reduction of Mn(III) and Mn(IV) oxide minerals. In turn, these oxides are attributed to the aerobic oxidation of Mn(II) in the presence of oxygen. Molecular clock models are used to independently date the evolution of the crown group cyanobacteria and have produced estimates that range from before 3 billion years ago to after the GOE, depending on the sequence datasets used, prior assumptions made and specific model calibrations[26]. These models support the radiation of anoxygenic green sulfur bacteria (such as *Chlorobium*) and green non-sulfur bacteria after the GOE[26], but also show that stem-group green sulfur bacteria diverged as early as 2.9 billion years ago. Given that the last common ancestor of modern green sulfur bacteria was photosynthetic, model estimates are consistent with anoxygenic photosynthesis within stem-group green sulfur bacteria long before the GOE (Extended Data Fig. 6). Therefore, anaerobic manganese oxidation that requires anoxygenic photosynthetic activity in the presence of sulfide could be as old as the anoxygenic phototrophic ancestors of any extant groups of phototrophs (including green sulfur bacteria, cyanobacteria or even an extinct lineage of anoxygenic phototrophs). Because any of these scenarios can pre-date the GOE, the relative contributions of anaerobic and oxygen-dependent Mn(II) oxidation to the redox texture of sedimentary rocks much before the GOE[27] are an open question, and the loss of mass-independent sulfur isotope signals at the GOE[28] remains the firmest evidence for the biological production of oxygen.

Online content

Any methods, additional references, Nature Research reporting summaries, source data, extended data, supplementary information, acknowledgements, peer review information; details of author contributions and competing interests; and statements of data and code availability are available at https://doi.org/10.1038/s41586-019-1804-0.

1. Planavsky, N. J. et al. Evidence for oxygenic photosynthesis half a billion years before the Great Oxidation Event. *Nat. Geosci.* **7**, 283–286 (2014).
2. Crowe, S. A. et al. Atmospheric oxygenation three billion years ago. *Nature* **501**, 535–538 (2013).
3. Tebo, B. M. et al. Biogenic manganese oxides: properties and mechanisms of formation. *Annu. Rev. Earth Planet. Sci.* **32**, 287–328 (2004).
4. Oze, C., Sleep, N. H., Coleman, R. G. & Fendorf, S. Anoxic oxidation of chromium. *Geology* **44**, 543–546 (2016).
5. Liang, M.-C., Hartman, H., Kopp, R. E., Kirschvink, J. L. & Yung, Y. L. Production of hydrogen peroxide in the atmosphere of a Snowball Earth and the origin of oxygenic photosynthesis. *Proc. Natl Acad. Sci. USA* **103**, 18896–18899 (2006).
6. Dismukes, G. C. et al. The origin of atmospheric oxygen on Earth: the innovation of oxygenic photosynthesis. *Proc. Natl Acad. Sci. USA* **98**, 2170–2175 (2001).
7. Johnson, J. E. et al. Manganese-oxidizing photosynthesis before the rise of cyanobacteria. *Proc. Natl Acad. Sci. USA* **110**, 11238–11243 (2013).
8. Culver, D. A. & Brunskill, G. J. Fayetteville Green Lake, New York. V. Studies of primary production and zooplankton in a meromictic marl lake. *Limnol. Oceanogr.* **14**, 862–873 (1969).
9. Pavlov, A. A. & Kasting, J. F. Mass-independent fractionation of sulfur isotopes in Archean sediments: strong evidence for an anoxic Archean atmosphere. *Astrobiology* **2**, 27–41 (2002).
10. Daye, M., Higgins, J. & Bosak, T. Formation of ordered dolomite in anaerobic photosynthetic biofilms. *Geology* **47**, 509–512 (2019).
11. Anbar, A. D. & Holland, H. D. The photochemistry of manganese and the origin of banded iron formations. *Geochim. Cosmochim. Acta* **56**, 2595–2603 (1992).
12. Beukes, N. J. Facies relations, depositional environments and diagenesis in a major early Proterozoic stromatolitic carbonate platform to basinal sequence, Campbellrand Subgroup, Transvaal Supergroup, Southern Africa. *Sedim. Geol.* **54**, 1–46 (1987).
13. Pibernat, I. V., IV & Abella, C. A. Sulfide pulsing as the controlling factor of spinae production in *Chlorobium limicola* strain UdG 6038. *Arch. Microbiol.* **165**, 272–278 (1996).
14. Ha, P. T. et al. Syntrophic anaerobic photosynthesis via direct interspecies electron transfer. *Nat. Commun.* **8**, 13924 (2017).
15. Prince, R. C. & Olson, J. M. Some thermodynamic and kinetic properties of the primary photochemical reactants in a complex from a green photosynthetic bacterium. *Biochim. Biophys. Acta* **423**, 357–362 (1976).
16. Dasgupta, J., Tyryshkin, A. M., Kozlov, Y. N., Klimov, V. V. & Dismukes, G. C. Carbonate complexation of Mn^{2+} in the aqueous phase: redox behavior and ligand binding modes by electrochemistry and EPR spectroscopy. *J. Phys. Chem. B* **110**, 5099–5111 (2006).
17. Butterfield, C. N., Soldatova, A. V., Lee, S.-W., Spiro, T. G. & Tebo, B. M. Mn(II,III) oxidation and MnO_2 mineralization by an expressed bacterial multicopper oxidase. *Proc. Natl Acad. Sci. USA* **110**, 11731–11735 (2013).
18. Geszvain, K., Smesrud, L. & Tebo, B. M. Identification of a third Mn(II) oxidase enzyme in *Pseudomonas putida* GB-1. *Appl. Environ. Microbiol.* **82**, 3774–3782 (2016).
19. Andeer, P. F., Learman, D. R., McIlvin, M., Dunn, J. A. & Hansel, C. M. Extracellular haem peroxidases mediate Mn(II) oxidation in a marine *Roseobacter* bacterium via superoxide production. *Environ. Microbiol.* **17**, 3925–3936 (2015).
20. Hemp, J. et al. Genomics of a phototrophic nitrite oxidizer: insights into the evolution of photosynthesis and nitrification. *ISME J.* **10**, 2669–2678 (2016).
21. Hulth, S., Aller, R. C. & Gilbert, F. Coupled anoxic nitrification/manganese reduction in marine sediments. *Geochim. Cosmochim. Acta* **63**, 49–66 (1999).
22. Kurzweil, F., Wille, M., Gantert, N., Beukes, N. J. & Schoenberg, R. Manganese oxide shuttling in pre-GOE oceans—evidence from molybdenum and iron isotopes. *Earth Planet. Sci. Lett.* **452**, 69–78 (2016).
23. Ossa Ossa, F., Hofmann, A., Vidal, O., Kramers, J. D. & Cavalazzi, G. Unusual manganese enrichment in the Mesoarchean Mozaan Group, Pongola Supergroup, South Africa. *Precambr. Res.* **281**, 414–433 (2016).
24. Beukes, N. J., Gutzmer, J. & Nel, B. Ce anomalies in similar to 2.4 Ga iron and manganese formations as proxy for early oxygenation of oceanic environments. *Geochim. Cosmochim. Acta* **74**, A85 (2010).
25. Manikyamba, C. & Naqvi, S. M. Geochemistry of Fe–Mn formations of the Archaean Sandur schist belt, India – mixing of clastic and chemical processes at a shallow shelf. *Precambr. Res.* **72**, 69–95 (1995).
26. Magnabosco, C., Moore, K. R., Wolfe, J. M. & Fournier, G. P. Dating phototrophic microbial lineages with reticulate gene histories. *Geobiology* **16**, 179–189 (2018).
27. Hazen, R. M. et al. Mineral evolution. *Am. Mineral.* **93**, 1693–1720 (2008).
28. Bekker, A. et al. Dating the rise of atmospheric oxygen. *Nature* **427**, 117–120 (2004).

Methods

Culturing and sequencing

Enrichment and culturing conditions. Sediments were retrieved from Fayetteville Green Lake (FGL) by a metallic gravity scoop and stored at 4 °C in fully filled, hermetically sealed glass jars. These samples were used as inoculum for enrichment cultures in the FGL medium. All inoculations were conducted in an anaerobic chamber under a 5%CO_2/5%H_2/balN_2 (v/v/v) atmosphere using standard anaerobic techniques[29]. In brief, FGL medium was flushed before and after autoclaving in hermetically sealed glass bottles. Sterile flushed FGL medium was inoculated inside the anaerobic chamber (5%CO_2/5%H_2/balN_2 (v/v/v) atmosphere). To avoid any issues associated with the exposure of biofilms to H_2, the serum bottles were opened inside the anaerobic chamber, inoculated in about 1 min, closed immediately, capped and flushed again with CO_2/N_2 for 60–75 min to remove H_2. All experiments were conducted in batch cultures and all cultures were inoculated by approximately 1 mg of biofilm that had been washed 6 times by anoxic nanopure water[30,31], mechanically dispersed by passing through a syringe and resuspended in sterile anaerobic medium. All these steps were carried out in the anaerobic glove box. All enrichment cultures were incubated at 27 °C with an incandescent white light bulb and a 12:12-h day:night cycle. All plasticware used in the anaerobic chamber was introduced into the chamber at least one week before the experiments.

The culture medium (FGL medium) contained 0.1 mM KH_2PO_4, 5.61 mM NH_4Cl, 0.9 mM KCl, 0.024 M $NaHCO_3$, 1 mM $MnCl_2{\cdot}2H_2O$, 1 mM Na_2SO_4 and 1 ml/l of trace element solution. The trace element solution was prepared in 10% (v/v) HCl and contained, per litre, 1.5 g $FeCl_2{\cdot}4H_2O$, 190 mg $CoCl_2{\cdot}6H_2O$, 100 mg $MnCl_2{\cdot}4H_2O$, 70 mg $ZnCl_2$, 31 mg Na_2MoO_4, 6 mg H_3BO_3, 2 mg $CuCl_2{\cdot}2H_2O$. The pH of the medium was adjusted to 7 by the addition of NaOH (1 M) or HCl (1 M). After adjusting the pH to 7, the FGL medium was distributed into glass bottles of different volumes (12, 25, 50, 150 and 200 ml). The final background concentration of manganese was 0.4 μM. To inhibit the growth of oxygenic phototrophs, we added 0.01 mM 3-(3,4-dichlorophenyl)-1,1-dimethylurea (DCMU) to the initial enrichments. All analyses described in the main text used later enrichments that were grown in DCMU-less medium. Glass serum bottles were capped by butyl rubber stoppers and aluminium seals. Before autoclaving, the FGL medium in bottles was flushed by 20% CO_2:80% N_2 for 1 h, the serum bottle headspaces for another 40 min total. The bottles were then autoclaved (40-min sterile). After autoclaving, the FGL medium in bottles were flushed again by 20% CO_2: 80% N_2 for one hour, the serum bottle headspaces for another 40 min total after cooling.

A separately prepared selenium stock solution contained 2 mg of Na_2SeO_3 in 1,000 ml of 0.01 M NaOH. This solution was autoclaved and made anaerobic by flushing the bottles for 1 h and 40 min with 20% CO_2:80% N_2. The vitamin solution was prepared in nanopure water by aerobic filter sterilization and contained, per litre, 2 mg biotin, 2 mg folic acid, 10 mg pyridoxine–$2H_2O$, 5 mg thiamine–HCl–$2H_2O$, 5 mg riboflavin, 5 mg nicotinic acid, 5 mg D-Ca–pantothenate, 0.1 mg vitamin B12, 5 mg *p*-aminobenzoic acid and 5 mg lipoic acid.

The master stock solution (20×) contained 1.5 mM $MgCl_2{\cdot}6H_2O$, 1 mM $CaCl_2{\cdot}2H_2O$, 1 ml of vitamin solution and 1 ml of the selenium stock solution in 50 ml nanopure water. The master solution was filter-sterilized and flushed for 1 h and 40 min by 20% CO_2:80% N_2 gas mixture. This solution was added to the FGL medium immediately before inoculation, 5 ml per 100 ml medium. Manganese was added at the time of inoculation from concentrated anaerobic stock solution of $MnCl_2{\cdot}4H_2O$ (1 M). Finally, after inoculation, the medium was reduced by the addition of sulfide from a concentrated anaerobic stock solution of $Na_2S{\cdot}5H_2O$ (0.2 M).

The medium used for the initial enrichment was reduced by the addition of 4 mM sodium ascorbate instead of sulfide, to minimize the growth of organisms that require high concentrations of sulfide as an electron donor. A brown microbial mat formed on the surface of the inoculated sediments after 3–4 weeks. Fragments of this mat were transferred into the sterile medium with the same composition as described above, incubated in the same conditions for one month and transferred again. Most experiments described here used biofilms that had undergone at least four transfers from the initial enrichment.

Modified FGL medium. All experiments described in the main text used the modified basal FGL (MFGL) medium. This medium did not contain DCMU, sulfate or ascorbate, and was reduced by 20–50 μM Na_2S. Sterile MFGL contained only traces of sulfate (<0.9 μM), nitrate (<0.5 μM) and nitrite (<0.1 μM), as detected by ion chromatography (see 'Concentrations of dissolved species in culture media').

To evaluate the influence of light on growth, biofilms from the third transfer were inoculated into the MFGL medium. One triplicate set of batch cultures was incubated for 2 weeks in the light at 27 °C at a distance of 35 cm from an incandescent white light bulb that emits between 400–700 nm. Another set was incubated at the same time and at the same temperature but was shielded from the light by aluminium foil.

To reduce the carryover of manganese oxides in the biofilm inoculum, we reduced the inoculums using a previously described protocol[32]. In brief, microbial biofilms that had been grown in the presence of light and 1 mM Mn(II) were collected and incubated in anaerobic sterile ascorbic acid (0.25 mM) in the anaerobic chamber for 10 min. After this incubation, the biofilms were washed three times with sterile, anaerobic nanopure water. XRD analyses of biofilms treated in this manner showed that this protocol removed manganese oxide minerals but increased the abundance of elemental sulfur in the inoculum. Elemental sulfur was absent from the biofilms before the treatment.

To characterize the effect of different initial concentrations of manganese and sulfide on mineral precipitation, biofilms from the third transfer of the original enrichment culture were inoculated into the MFGL medium amended by $MnCl_2$, and Na_2S from 0.5 M and 0.1 M anaerobic stock solutions. All stock solutions were prepared, autoclaved and stored under an atmosphere of N_2. The effect of manganese concentration on manganese oxidation was evaluated in three sets of triplicate inoculated cultures that contained 0.1, 1 or 5 mM $MnCl_2$. All these cultures were reduced with 50 μM Na_2S. The effect of H_2S concentration on manganese oxidation was explored in three sets of triplicate cultures reduced by 0.05, 0.25 or 1 mM of Na_2S, all amended with 1 mM $MnCl_2$. An additional set of triplicate cultures contained 1 mM Mn(II) and 0.02 mM Na_2S. All cultures were incubated for two weeks.

Further enrichment of manganese-oxidizing and sulfide-oxidizing microorganisms. Microbial communities capable of anaerobic oxidation of manganese were further enriched by inoculating anaerobically sealed agar shake tubes with the dispersed biofilms, serially diluting the cultures in agar, transferring colonies into liquid medium and repeating the entire process for a second time[33,34]. The MFGL medium in agar shake tubes was solidified by 1.1% agar. Biofilms were washed with anaerobic nanopure water in the anaerobic glove box and mechanically dispersed in 10 ml of the basal MFGL medium. The first agar shake tube was inoculated with 10% (1 ml) of the dispersed inoculum and diluted by 5 successive transfers of 1 ml into 9 ml of sterile MFGL.

The additions of sulfide and manganese to the basal MFGL in agar shake tubes targeted two different conditions: condition (1), 0.02 mM Na_2S and 1 mM $MnCl_2$, sought to enrich for microorganisms that can photosynthesize in the presence of low sulfide concentrations and oxidize Mn(II); and condition (2), 1 mM Na_2S ($MnCl_2$ added only in the trace metal solution), enriched for *Chlorobium* spp. that can oxidize sulfide. Extended Data Table 2 summarizes the enrichment protocol and conditions. The shake tubes were incubated at 27 °C at a distance of 35 cm from the incandescent white light bulb. Colonies that formed after one month were transferred from the solid medium into the liquid

medium that contained the same concentrations of $MnCl_2$ and Na_2S. Biofilms that grew in liquid after one month were mechanically dispersed by a syringe, inoculated into another set of agar shake tubes and incubated for one month. Colonies from the shake tubes were inoculated again into the liquid medium. The purity of the cultures at each transfer was tested by Sanger sequencing. Amplified 16S rRNA genes were sequenced in both directions using either 27F (5′- AGAGTTTGATCCTGGCTCAG-3′) or 1492R (5′-ACG GCT ACC TTG TTA CGA CTT-3′) (Integrated DNA Technologies), assembled to get a nearly full-length 16S rRNA gene (GeneWiz) and identified using nucleotide BLAST on GeneBank[35]. Future experiments should also explore the possibility of light-dependent production of organoperoxides in the medium as a function of vitamins and Fe(II) in the medium.

DNA extraction, 16S rRNA gene Illumina sequencing and phylogenetic analyses. A 500-µl sample of each biofilm enrichment (including early enrichments and the lake inoculum) was collected and spun down into a pellet. Total DNA was extracted from samples using the PowerSoil DNA Isolation Kit (MoBio) according to manufacturer's instructions and eluted in 60 µl C6 solution. Upon extraction, DNA was quantified using NanoDrop (Thermo Scientific). The extracted samples and blank-template controls from the PowerSoil DNA Isolation kit were stored at −80 °C and sent to Argonne National Laboratory on dry ice for sequencing. The community composition was characterized using 16S rRNA gene amplicon paired-end sequencing on the MiSeq Illumina platform. In brief, V4 region of the 16S rRNA gene (515F–806R) from each sample was amplified using the bacterial-specific primers 515F (5′-GTGCCAGCMGCCGCGGTAA-3′) and 806 R (5′-GGACTACHVGGGTWTCTAAT-3′)[36]. After the amplifications, the PCR amplicons were quantified using Quant-iT PicoGreen dsDNA Assay Kit (ThermoFisher/Invitrogen, P11496) according to manufacturer's instructions and pooled in equal concentrations (240 ng) to a single tube. This pool was cleaned up using MoBio UltraClean PCR Clean-Up Kit (MoBio) and quantified using the Qubit (Invitrogen). The pooled samples were sequenced on the Illumina MiSeq platform (Illumina). All library preparations, pooling, quality controls and sequencing runs were performed at the Argonne National Laboratory. Sequence data were analysed using QIIME v.1.9.0[37]. Paired-end reads were joined using fastq-join method[38], and libraries were demultiplexed and filtered. Any reads that did not assemble by perfect matches in the overlapping region or meet the *q*-score (>20) threshold were removed and were not used in subsequent analyses. Chimeric sequences were identified using UCHIME's usearch61 de novo-based chimaera detection algorithm[39] and removed from the quality-filtered sequences. Filtered and chimaera-free sequences were aligned and clustered into operational taxonomic units at >97% similarity level using closed-reference UCLUST algorithm against the Greengenes v.13.8 reference dataset as a database[40]. The most abundant sequence from each cluster was selected as a representative sequence. All representative sequences were aligned using PyNAST[37]. A phylogenic tree for subsequent phylogenetic analyses was built using FastTree[41]. Operational taxonomic unit counts were rarified to 10,000 sequences per sample for diversity analysis using taxonomic and phylogenetic indices that included the Shannon and Faith's PD index. To identify bacterial taxa with sequences that are more abundant in samples grown in light and/or with Mn(II), we used LEfSe, which performs a nonparametric Wilcoxon sum-rank test followed by linear discriminant analysis (LDA), coupled with effect size measurements to assess differentially abundant taxa[42]. *Chlorobium* sp. sequences were significantly enriched in samples grown in the presence of light and Mn(II) with LDA scores >5. Cultures grown in light had significantly more *Chlorobium* sp. (analysis of varaiance (ANOVA), $F = 23.4521$, df factor = 5, df error = 12, $P < 0.0001$; Tukey's HSD, $P < 0.01$). Sequence data are available as FASTQ files at the National Center for Biotechnology Information (NCBI) via Sequence Read Archive (SRA), under the SRA accession ID number SRP133329.

Metagenome sequencing and analysis. To determine the metabolic potential of cultures grown from colonies that targeted specific growth conditions (see ' Further enrichment of manganese-oxidizing and sulfide-oxidizing microorganisms'), we sequenced their metagenomes. The DNA of enrichments obtained using condition (1) was extracted using a modified phenol–chloroform method with ethanol precipitation as previously described[43] and quantified by a Qubit 2.0 Fluorometer (Thermo Fisher Scientific). This DNA was sent for metagenomic sequencing to the University of Southern California's Genome and Cytometry Core Facility. The library preparation, quality control and sequencing were performed at the Cytometry Core Facility. In brief, before sequencing on the Illumina HiSeq 2500 platform, DNA was sheared using dsDNA Shearas Plus (Zymo), cleaned up using Agencourt AMPure XP beads (Beckman-Coulter), the library was quantified using the Qubit 2.0 Fluorometer and the DNA fragment size was determined with an Agilent Bioanalyzer 2100.

The quality control of the sequence data was performed using Trimmomatic v.0.36 using default parameters and a minimum sequence length[44] of 36 bp. IDBA-UD v.1.1.2. was used to assemble the reads with a 2,000 bp minimum contig length. SAMtools v.1.3.1[45] was used to convert files to binary format for downstream analysis. VizBin was used to delineate individual genomes from the enrichment metadata[46] and the genomes were assigned putative taxonomic identities according to their placement in a phylogenetic tree in CheckM v.1.0.4 using the 'tree' command[47].

Individual genomes obtained from the metagenome data were submitted to the DOE Joint Genome IMG-MER (Integrated Microbial Genomes) pipeline for gene calling and assembly[48]. The protein-coding-gene prediction tool Prodigal v.3.0.0 was used to determine genes in the enrichment grown from the colony on 1 mM $MnCl_2$ and 20–50 µM Na_2S. The genome of *C. limicola* was 98.4% similar to *C. limicola* Frassasi[49].

To detect putative Mn(II)-oxidizing genes in *C. limicola*, we first generated a blast database of protein-coding Mn(II)-oxidizing genes by selecting genes that encode for multi-copper oxidases and animal haem peroxidases. Because multi-copper oxidases and animal haem peroxidases each contain several classes of enzymes and can transfer electrons from a number of different substrates, we focused on enzymes with confirmed manganese-oxidizing activities by biochemical and molecular assays. All multi-copper oxidases and animal haem peroxidases involved in Mn(II) oxidation and characterized to date are from aerobic microorganisms and include genes such as *mnxG*, *mcoA* and *mopA* in *Pseudomonas putida*[18], *mnxG* in the spores of *Bacillus* strain SG-1[19], *moxA* in *Pedomicrobium* sp. ACM 3067[50], and *mopA* in *Aurantimonas manganoxydans* SI85-9A1[51] and *Roseobacter* sp. AzwK-3b[19]. To determine whether *Chlorobium* has any homologues with characterized manganese-oxidizing multi-copper oxidases and animal haem peroxidases, we used BLASTp[52] and queried translated Mn(II)-oxidizing genes against the *Chlorobium* genome with an *e*-value cut-off of 10^{-5} and a bit score of 30. Homologues of multi-copper oxidases and animal haem peroxidases in *C. limicola* are shown in Extended Data Table 4.

Sequence data for *C. limicola* can be accessed at the JGI-IMG under IMG submission ID 124328.

Spectroscopy

X-ray photoelectron spectroscopy. X-ray photoelectron spectroscopy (XPS) was performed on a K-alpha + X-ray photoelectron spectrometer (K-Alpha + XPS, Thermo Fisher). Biofilms were collected and centrifuged at 14,000 rpm for 5 min in the anaerobic chamber to form pellets. The pellets were placed on double-sided carbon tape and dried in the anaerobic chamber. To maintain the anoxic conditions, the samples were stored in the anaerobic chamber in hermetically sealed glass vials before analysis. All samples were fractured in high vacuum (3×10^{-8} Torr) in the outer pressure chamber and then moved directly

into the main XPS measurement chamber. An incident monochromatic X-ray beam from the Al K Alpha target (15 kV, 10 mA) was focused on a 0.4 mm × 0.3-mm area of the surface at a 45° angle with respect to the sample surface. Depth profile etching with an etch cycle of 30 s and a total of 10 levels yielded high-resolution spectra. The electron energy analyser perpendicular to the sample surface was operated with a pass energy of 50 eV to obtain XPS spectra at a 0.1-eV step size and a dwell time of 50 ms. Each peak was scanned 15 times. To ensure representative data from heterogeneous samples, we probed a total of 50–80 points per sample. XPS data were treated and analysed using CasaXPS curve resolution software package. Spectra were best fit after Shirley background subtractions by nonlinear least squares CasaXPS curve resolution software package. Gaussian and Lorentzian contributions to the line shapes were numerically convoluted using a Voigt function. The different XPS lines with sets of Gaussian and Lorentzian peaks were empirically fitted with different standards corresponding to different oxidation sets (MnO, $MnCO_3$, Mn_2O_3, Mn_3O_4, MnO_2 and $MnCaO_3$). Each manganese XPS spectrum was empirically best fitted with multiple standard phases (MnO, $MnCO_3$, Mn_2O_3, Mn_3O_4, MnO_2 and $MnCaO_3$) that produced the minimum residual. The average fit properties for all treated spectra were acceptable as the following: $R_{expected} = 1.60$, $R_{profile} = 1.71$, significance level = 0.05, residual s.d. = 1.67, goodness of fit = 1.78, critical $\chi^2 = 3.84$.

Interpretation of XPS spectra. The redox state of manganese in microbial cultures was confirmed by XPS (Extended Data Fig. 3). The Mn2*p* XPS spectra of the dark culture exhibited two major peaks at binding energies of 640.90 eV and 652.2 eV, which correspond to $Mn2p_{2/3}$ and $Mn2p_{1/2}$, respectively. This is consistent with other reports[53,54] on Mn(II) phases of Mn. In the photosynthesizing culture, the Mn2*p* peak shifted to a high-energy side and the intense satellite peak characteristic of Mn(II) diminished. These biofilms contained manganese in different valence states. At some analysed spots, the Mn2*p* XPS spectrum exhibited two major peaks of $Mn2p_{2/3}$ and $Mn2p_{1/2}$ at binding energies of 642 eV and 653 eV, respectively. These correspond to Mn(IV) in calcium–manganese oxide phases[55]. Peaks at $Mn2p_{2/3}$ with binding energies 641.61 eV and 641.47 eV, respectively, were also detected. These peaks correspond to Mn(III) in Mn_2O_3 and Mn(III) and Mn(II) in Mn_3O_4 phases[56,57].

The redox state of the manganese in the culture enriched in condition (1) and condition (2) was confirmed by XPS (Extended Data Fig. 4). The Mn2*p* XPS spectra of this culture (Extended Data Fig. 4a) exhibited two major peaks at binding energies of 641.41 eV and 653.15 eV, corresponding to $Mn2p_{2/3}$ and $Mn2p_{1/2}$, respectively, and matching the peaks[58,59] of Mn_3O_4. The Mn2*p* XPS spectra of the condition (2) enrichment (Extended Data Fig. 4b) exhibited $Mn2p_{2/3}$ peaks at 640.97 eV and 652.2 eV, which correspond to $Mn2p_{2/3}$ and $Mn2p_{1/2}$, respectively. This is consistent with other reports of MnO phases[56,58].

Probing the redox state of manganese in biofilms. We used XPS to detect oxidized manganese in colonies enriched on 1 mM Mn(II) (condition (1)). Extended Data Table 3 summarizes the procedure used to study the Mn(II) oxidation activity in the enrichment cultures. Manganese oxidation was tested using cultures that were enriched as colonies in agar shake tubes (condition (1) and condition (2)) (see Extended Data Table 3 and 'Spectroscopy' and 'Interpretation of XPS spectra'). Biofilms from condition (1) were grown in duplicate 10-ml cultures with 1 mM $MnCl_2$ and 0.02 mM Na_2S, mechanically dispersed and resuspended into separate 10-ml liquid solutions. Five per cent v/v of this suspension was transferred into 10 ml of MFGL medium with 1 mM $MnCl_2$ and 0.02 mM Na_2S and the cultures were incubated at 27 °C for 1 week before the assay. A second assay tested the Mn(II) oxidation activity without requiring the very sparse biofilm to grow. The condition (1) enrichment was grown for two weeks as described in 'Probing the redox state of manganese in biofilms', centrifuged at 8,000 rpm in the anaerobic chamber, washed 3 times with anaerobic water and transferred into 10 ml of MFGL with 1 mM $MnCl_2$ and 0.02 mM Na_2S. These cultures were incubated for 3 days in a 12:12 h light:dark regime and collected anaerobically. This procedure preserved the cell density of the original biofilms and did not require microbial growth.

To test for Mn(II) oxidizing activity in the enrichment from condition 2 (*Chlorobium* sp. and *Desulfomicrobium* sp.), the culture was grown in 10 ml of the basal MFGL amended with 1 mM Na_2S, collected anaerobically and dispersed in 10 ml of the basal MFGL medium. This suspension was used to inoculate 10 ml of the basal MFGL amended with 1 mM $MnCl_2$ and 0.02 mM Na_2S at 5% v/v. The inoculated medium was incubated in the light/dark regime for one week. To test for Mn(II) oxidizing activity without requiring the low-biomass biofilms to grow, the enrichment from condition (2) was grown for 2 weeks in 10 ml of the basal MFGL amended with 1 mM Na_2S, centrifuged at 8,000 rpm in the anaerobic chamber, washed 3 times with anaerobic water and transferred to 10 ml of MFGL with 1 mM $MnCl_2$ and 0.02 mM Na_2S. These cultures were incubated for 3 days in the 12:12 h light:dark regime and collected anaerobically. All collected microbial pellets were dried on carbon tape and stored anaerobically inside serum bottles with N_2 atmosphere and placed inside the anaerobic chamber in the dark at 26 °C until XPS analysis.

Probing the redox state of manganese in co-cultures. *C. limicola* (DSM 245, DSMZ) and *C. tepidum* (DSM 12025, DSMZ) were inoculated with 5% v/v inoculum and grown in 50 ml MFGL medium supplemented with 0.05 mM Na_2S and 0.5 g/l yeast extract in a 12:12 h light:dark regime at 27 °C for 3 weeks. *G. lovleyi* (DSM 17278, DSMZ) was grown in MFGL supplemented with 2.8 mM ferrihydrite and 5 mM acetate and reduced with 0.05 mM Na_2S in the dark at 21 °C for 3 weeks. Microorganisms from these cultures were inoculated as 5% v/v inoculum in the following combinations: *C. limicola* + *C. tepidum*, *C. tepidum* + *G. lovleyi*, *C. limicola* + *G. lovleyi* and *C. limicola* + *C. tepidum* + *G. lovleyi*. All these co-cultures were grown in 10 ml MFGL medium with 1 mM Mn(II) and 0.05 mM Na_2S in a 12:12 h light:dark regime at 27 °C for 2 weeks. The biomass was collected anaerobically, the pellets were dried on carbon tape and stored anaerobically under N_2 inside the anaerobic chamber in the dark at 26 °C until XPS analysis. The oxidation state of manganese was characterized by XPS in all four cultures.

X-ray powder diffraction

XRD patterns were obtained in reflection mode with Ni-filtered Cu Kα radiation ($\lambda = 1.5406$ Å) as X-ray source on an X'Pert PRO diffractometer (XRD, X'Pert PRO, PANalytical) equipped with an X'Celerator detector (PANalytical). The patterns were measured in 2θ range from 3° to 90° with a scanning step of 0.008° and a fixed counting time of 600 s at 45 kV and 40 mA. Biofilms were collected and centrifuged at 14,000 rpm for 5 min in the anaerobic chamber. Microbial paste was smeared on Zero Diffraction Disk (23.6-mm diameter × 2.0-mm thickness, Si crystal, MTI) and dried in the anaerobic chamber. The samples were analysed inside the anaerobic dome to maintain the anoxic conditions during the XRD analyses. Data were analysed and fitted using High Score Plus program version 4.5. The average fit properties for all treated spectra were acceptable as the following: residual s.d. = 1.63, $R_{expected} = 1.28$, $R_{profile} = 1.63$, significance level = 0.05, goodness of fit = 1.69, critical $\chi^2 = 3.84$.

Precipitated minerals were also analysed using in-situ synchrotron-based XRD at the Advanced Light Source at the beamline 12.3.2. Biofilms were collected on site and the biofilm paste was loaded into transmission sample XRD cells. The transmission synchrotron diffraction data were collected using a DECTRIS Pilatus 1M hybrid pixel area detector placed at an angle 2θ of 35° at approximately 170 mm from the sample. The 4-bounce monochromator was set to an energy was 10 keV ($\lambda = 1.239842$ Å). The sample geometry with respect to the incident beam and the detector was carefully calibrated using Al_2O_3 powder. The 2D diffraction patterns (Fig. 1d) were analysed and integrated along the

azimuthal direction into 1D diffractograms using the X-ray microdiffraction analysis software (XMAS v6) developed at the Advanced Light Source for the Advanced Light Source beamline 12.3.2, and Matlab R2017a.

Determination of XRD detection limit. To determine the detection limit of XRD, 0.05, 0.01, 0.02, and 1 mg of MnO_2 was mixed with 10 mg of dry anaerobic biofilm that did not contain green sulfur bacteria or manganese oxides and spread on Zero Diffraction Disk (23.6-mm diameter × 2.0-mm thickness, Si crystal, MTI). The mixtures were analysed by X'Pert PRO diffractometer XRD, X'Pert PRO, PANalytical) equipped with an X'Celerator detector (PANalytical) over 10-h analysis time. MnO_2 standard and the bacterial biofilm were also run separately as controls. The detection limit of XRD was determined by the mass of MnO_2 that yielded discernible diffraction peaks in the XRD spectrum.

Interpretation of XRD peaks. The XRD spectra of microbial cultures incubated in the light with Mn(II) (Fig. 2) showed peaks that can be indexed to a ternary manganese oxide; $CaMnO_3$ (ICDD-01-016-2217) with lattice constants of a = 5.2917 nm, b = 7.4803 nm and c = 5.2870 nm[58]. $CaMnO_3$ is not known to occur naturally.

Dolomite was the most abundant phase in the cultures and its peaks were indexed as (104), (101), (110), (11-3), (202) and (018) (ICDD-04-011-9833). The absence of light inhibited the growth of photosynthetic microorganisms and the formation of manganese-oxide minerals, and also reduced the precipitation of dolomite (Fig. 2). Biofilm incubated in the dark showed the precipitation of calcium carbonate phase, $CaCO_3$ (ICDD-00-058-0471) indexed for (121) and (102). In addition to the various carbonate phases, the XRD spectrum showed two different phases of elemental sulfur (S^0); (ICDD-04-020-2294) indexed for (110), (−101) and (−211) and (ICDD-05-001-0219) indexed for (110) and (−101).

The XRD spectra of microbial cultures incubated at different concentrations of manganese and sulfur showed peaks of manganese oxide, dolomite and elemental sulfur (Extended Data Fig. 2). The latter formed in microbial cultures that were incubated with 0.25–1 mM H_2S and in the cultures grown with less than 1 μM Mn(II) (see the composition of the trace metal solution in 'Enrichment and culturing conditions'). S^0 (ICDD-05-001-0219), was indexed for (110), (−101), (011) and (−211).

Microscopy

Scanning electron microscopy. Scanning electron micrographs were acquired by a Zeiss Merlin scanning electron microscope with the GEMINI II column (Zeiss Merlin SEM, Carl Zeiss microscopy). The microscope was equipped with a field gun emission and energy-dispersive X-ray spectrometer (EDS, EDAX detector; EDAX) that operated at an accelerating voltage of 5–15 kV, probe current of 100 pA and a working distance of 8.5 mm. On-axis in-lens secondary electron detector was used during imaging. The samples were fixed by 0.2 M sodium cacodylate, 0.1% $CaCl_2$ and 2.5% glutaraldehyde in anaerobic water for 2–3 days at 4 °C. The fixed samples were washed by 0.1 M sodium cacodylate followed by a wash in nanopure water. After washing, the samples were dehydrated in a series of ethanol–water solutions. The ethanol–water solution series included the following dehydration steps: 30% (20 min), 50% (20 min), 70% (20 min), 80% (20 min), 90% (20 min) and 100% (3 × 20 min) of 200 proof ethanol. After air-drying, the samples were mounted on double-sided carbon tape and coated with a thin layer 5 nm of Au/Pd or 10 nm of carbon using a Hummer V sputter coater. EDS spectra were treated and analysed by TEAM EDS 2.0 analysis software (EDAX) and Microsoft Excel 2016.

TEM. Transmission electron micrographs were obtained using FEI Tecnai F20 supertwin microscope (FEI Tecnai G2, FEI) with a 200-kV Schottky field emission gun. The samples were imaged at 80 kV with 1,024 × 1,024 CCD Gatan camera (Gatan). The samples were fixed by 0.2 M sodium cacodylate, 0.1% $CaCl_2{\cdot}6H_2O$ and 2.5% glutaraldehyde in aerobic nanopure water for 2–3 days at 4 °C. The samples were then washed with washing buffer (0.1 M sodium cacodylate in nanopure water), postfixed with 1% osmium tetroxide in water for 1 h, washed with aerobic nanopure water and stained with 1% uranyl acetate for 1 h. The stained samples were washed with nanopure water and dehydrated in an ethanol–water solution series. The ethanol–water solution series included the following dehydration steps: 30% (20 min), 50% (20 min), 70% (20 min), 80% (20 min), 90% (20 min), and 100% (3 × 20 min) of 200 proof ethanol. The samples were further dehydrated with propylene oxide:ethanol solvent (50:50, by vol) for 30 min, then with 100% propylene oxide. The epoxy resin used for embedding consisted of diglycerol ether of polypropylene glycol (EmBed 812, DER 736, Electron Microscopy Sciences, EMS no. 14130,), cycloaliphatic epoxide resin (ERL 4221 Electron Microscopy Sciences, EMS no. 14300), nonenyl succinic anhydride (NSA, Electron Microscopy Sciences, EMS no. 14300) and 2-(dimethylamino)ethanol (DMAE, Electron Microscopy Sciences, EMS no. 14300). The samples were embedded in resin and cut into 80-nm-thick sections with a diamond knife using Leica Reichert Ultracut E microtome (Reichert Ultracut E microtome, Leica) with a thickness setting of 50 nm. Thin sections were placed on FCF-200 grids (Electron Microscopy Sciences, FCF-200-Cu).

To determine whether the fixation and embedding protocols introduced any artefacts, photosynthetic biofilms were also collected without any further processing or staining in the anaerobic chamber. A drop of microbial culture was deposited on LC-200 grid (Electron Microscopy Sciences, LC-200-Cu) and imaged with JEOL 2010F TEM (JOEL 2010F, JOEL). The JEOL 2010F TEM is equipped with a Schottky field emission gun operating at 200 kV and a Gatan energy filter (GIF, Gatan 200, Gatan). The 2010F TEM has micro-diffraction, diffraction pattern in parallel beam and convergent beam electron diffraction features to allow SAED on selected mineral-encrusted bacteria with a high spatial resolution. Gold standard was used as reference for SAED analyses. The high-angle annular dark filed detector (Gatan) for atomic resolution scanning electron transmission microscopy in the free-lens control mode (STEM) and with an EDS (Bruker silicon drift detector SDD, Bruker) enabled elemental analysis at nanoscale resolution. Images in the TEM and STEM mode were taken by a digital camera (Gatan Orius, Gatan). SAED patterns were imaged using Gatan digiscan unit (Gatan). TEM, STEM and SAED images were recorded and treated using Gatan digital micrograph software (Gatan). EDS spectra were recorded and treated using INCA program (Oxford Instruments).

Interpretation of SAED patterns. Different types of manganese minerals in photosynthetic biofilms corresponded to different stages of mineral maturation. High-resolution TEM of the manganese oxide nanocluster surrounding a cell (Fig. 3) showed polycrystalline minerals with a uniform lattice fringe that corresponded to the (116) plane with interplanar spacing of 2.71 Å of calcium manganese oxide (ICDD-00-053-0092). The SAED patterns of minerals that were not associated with cell surfaces showed various minerals. One type of manganese mineral had four obvious polycrystalline diffraction rings that could be observed at 3.65 Å, 3.40 Å, 2.88 Å and 1.83 Å. These corresponded, respectively, to the (112), (211), (220) and the (323) crystal planes of Mn_3O_4 (ICDD-03-065-2776) (Fig. 3). Some globular nanocrystals of manganese oxide outside of any microbial surfaces (Fig. 3) showed lattice fringes with the interplanar spacing of 2.26 Å. This matched the characteristic interplanar spacing of the (200) plane of manganese oxide type MnO mineral (ICDD-04-004-3858).

Concentrations of dissolved species in culture media

Sulfide concentrations were determined using a modification of a previously published method[60] in samples of triplicate cultures for each time point. In brief, 200 μl of each liquid sample was diluted in 1 ml of 0.05 M zinc acetate. Standards were prepared from 1 mM anaerobic stock solution of Na_2S diluted by 0.05 M zinc acetate. The concentration of Na_2S

stock solution was verified by precipitating an exact volume of Na_2S with an excess volume of 0.3 M silver nitrate. Six hundred microlitres of the precipitated sample were transferred and reacted with 10 µl of diamine reagent. After 20 min reaction time in the dark, the absorbance was measured by a multi-mode reader spectrophotometer (BioTek, Synergy 2) at 670 nm.

The concentrations of sulfate, nitrite and nitrate in the samples of the liquid medium from triplicate cultures were determined by ion chromatography (Dionex ICS-16000 equipped with an auto-sampler Dionex AS-DV, Thermo Fisher), guard column (Dionex Ion Pac AG22, RFIC, Guard 2 × 50 mm, Thermo Fisher), analytical column (Dionex Ion Pac AS22, RFIC, Analytical 2 × 250 mm, Thermo Fisher, USA) and a trap column for metals (Dionex Ion Pac MFC-1, RFIC, trap column, metal free, 3 × 27 mm, Thermo Fisher). All samples were filtered anaerobically through 0.2-µm-pore-size filters (Acrodisc 25-mm syringe filter, PALL) and stored at −20 °C. The chloride ion was solid-phase extracted from all samples using a Ag/H cartridge (Dionex OnGuard II Ag/H, 2.5 c.c. cartridge, Thermo Fisher) before the analysis. The removal of the chloride ion affected the lower detection limit for phosphate, but not for sulfate and nitrate. The limits of detection for sulfate, nitrate and nitrite, respectively, were 20 µg/l, 20 µg/l and 10 µg/l respectively.

Total dissolved manganese concentrations in the liquid culture medium from triplicate cultures were determined by inductively coupled plasma-mass spectrometry (ICP-MS, Agilent 7500, Agilent). All samples were filtered through 0.2-µm-pore-size filters (Acrodisc 25-mm syringe filter, PALL), and acidified with 2% high purity HCl (hydrochloric acid 30%, Sigma Aldrich, suprapur- end Millipore, 100318) and stored at −20 °C. All samples were diluted with high-purity 2% HCl (hydrochloric acid 30%, Sigma Aldrich, suprapur- EMD Millipore, 100318) before the analysis.

Dissolved manganese in the liquid phase was also measured by leucoberbelin blue (LBB) assay[61] and iodometric method[62]. Oxidized manganese in the liquid phase includes any soluble valence state of manganese that can pass through the 0.2-µm pore filter. We used the iodometric method[62,63] to determine manganese oxidation state including Mn(II), Mn(III), Mn(IV) and Mn(VII). Again, none of the measurements detected oxidized manganese in the liquid phase. The LBB assay was also used to quantify the concentrations of oxidized manganese in biofilms. These concentrations were detected as oxidizing equivalents of $KMnO_4$ ('Quantification of biofilms and oxidized manganese in biofilms').

The concentration of peroxide was measured in triplicate samples of microbial biofilms and sterile controls incubated in the light with 1 mM Mn(II) and 50 µM Na_2S using a peroxidase activity assay kit (Sigma Aldrich, MAK092). The standard curve was measured using different dilutions of the H_2O_2 standard (Sigma Aldrich, MAK092C) in sterile culture medium mixed with the reaction mix composed of 2 µl fluorescent peroxidase substrate (Sigma Aldrich, MAK092B) and 48 µl of HRP positive control (Sigma Aldrich, MAK092D). A 100 µl of each diluted H_2O_2 standard and the samples were distributed into microplate wells. The plate was incubated at 37 °C and the initial measurement ($t_{initial}$) was measured after 3 min by multi-mode reader spectrophotometer (BioTek, synergy 2) at 570 nm. The absorbance was measured every 3 min until the value of the most-active sample exceeded the end linear range of the standard curve. We did not detect any H_2O_2 in the incubations or sterile controls. The limit of detection of H_2O_2 using colorimetric detection was 0.1 nM.

Quantification of biofilms and oxidized manganese in biofilms

The amount of biofilm was measured by crystal violet staining using a modification of a previously published assay[64]. In brief, biofilms from triplicate serum bottles were collected at each time point and centrifuged aerobically at 10,000 rpm for 30 min. The supernatant was decanted and 0.5 ml of 0.1% of aqueous crystal violet added (crystal violet, Sigma Aldrich, ACS reagent, ≥ 90% anhydrous basis, C6158). The stained biofilm was incubated in the dark at room temperature for 24 h, washed 15 times with nanopure water and air-dried. After drying, 0.5 ml of 30% acetic acid (37% acetic acid, Sigma Aldrich, ACS reagent, ≥ 99.7%, 695092) was added to the samples and left to react at room temperature for 30 min. Acetic acid solubilized all crystal violet molecules bound to peptidoglycan and exopolysaccharide. Thus, the solubilized crystal violet corresponds to the biomass in biofilms. The collected solubilized crystal violet was filtered through 0.2-µm-pore-size filters (Acrodisc 25-mm syringe filter, PALL) and 200 µl of the solution was transferred into a microtiter plate. The absorbance of the samples was measured at 550 nm using a spectrophotometer (BioTek, synergy 2).

Oxidized manganese in biofilms was quantified by the LBB assay. Biofilms were inoculated from frozen stocks into triplicate serum bottles that contained 25 ml or 50 ml of MFGL medium and incubated for one, two or three weeks. Biofilms from the frozen stock (about 5 mg) were washed 10 times with anaerobic nanopure water to remove any glycerol, inoculated into the culture medium and the medium was immediately flushed with 20% CO_2/80% N_2 (v/v) for 1 h. The biofilms grew for 2 weeks in the light, at which point, biofilms (about 5 mg) were transferred into serum bottles that each contained 25 ml of the fresh MFGL medium. Three bottles were incubated in the light, three in the dark and all biofilms were collected after one or two weeks by pipetting and centrifugation in the anaerobic glove box. After the LBB assay, all analysed samples were air-dried for >24 h and weighed. The one-week old biofilms weighed 16–18 mg; the two-week old biofilms weighed 19–21 mg. A separate experiment quantified the amount of oxidized manganese in duplicate 25-ml cultures of 3-week old biofilms that had been inoculated with about 0.1 mg of the washed material from frozen culture stocks and weighed <0.3 mg at the end of the experiment. In contrast to the experiments that yielded samples for XRD, XPS, scanning electron microscopy and TEM analyses, these experiments involved at most one successive transfer of biofilms after the inoculation from frozen stocks of biofilms enriched as described in 'Enrichment and culturing conditions'.

The working reagent was prepared as 0.04% LBB in 45 mM acetic acid and stored at 4 °C overnight in a light-proof container. Potassium permanganate ($KMnO_4$) 1 mM stock solution was freshly prepared in water and standards (5, 10, 15, 20, 40 and 50 µM) were prepared by diluting the stock solution in water. The samples were incubated for 20 min in 0.75 ml of the 0.04% LBB working reagent in the dark at room temperature and centrifuged for 90 s at 10,000 rcf to remove the biofilm and mineral particulates from the solution. The absorbance of the supernatant was measured on a spectrophotometer at 618 nm. To determine whether some manganese was oxidized in the dark, about 5 mg of the biofilm stock was inoculated into sterile MFGL in the dark for 2 weeks which detected on average 0.02 µM oxidizing equivalent per 5 mg of biofilm. Control experiments assayed the concentration of oxidized manganese in FGL enrichment cultures that contained 1 mM sulfide, and 1 mM $MnCl_2$ and did not detect any oxidized manganese.

Oxygen concentration

To determine how much oxygen can diffuse into the cultures through the butyl rubber caps, we used our in-house-developed oxygen sensor[65] based on the fluorescence lifetime[66] of 5,10,15,20-tetrakis(pentafluorophenyl)-21*H*,23*H*-porphinepalladium (II). The sensor can detect changes in the partial pressure of oxygen that are smaller than 1 µbar and its main sensitivity region[65] is 0–100 µatm.

Experiments were conducted to quantify the oxygen concentration in the cultures and the maximum amount of oxygen inflow. First, the partial pressures of oxygen in the headspaces of photosynthetic cultures, sterile controls incubated in the light and dark control cultures were measured automatically for 14 days. All serum bottles contained 100 ml of the medium reduced by 50 µM Na_2S (Extended Data Fig. 1). The partial pressure of oxygen in the headspaces of the bottles did not increase or fluctuate by more than 2 µbar over the course of the growth experiment. The main sources of noise were daily thermal fluctuations

(high-frequency component) and sensor aging (low-frequency component). The upper limit for the partial pressure of oxygen in the headspace is 2 µbar, measured in the beginning of the experiment. This partial pressure was lower than 0.5 µbar during most of the experiment. This corresponds to a maximum dissolved molecular oxygen concentration of 2.6 nM, assuming the equilibrium between O_2 in the headspace and O_2 dissolved in the culture medium according to Henry's law.

In an additional test, we incubated biofilms in the light in the anaerobic chamber under a 5%CO_2/5%H_2/balN_2 (v/v/v) atmosphere. The partial pressure of oxygen in the chamber was below 1 ppm, as opposed to 21% above the butyl rubber stoppers of the cultures that were incubated outside of the chamber. Therefore, orders-of-magnitude-less oxygen is expected to diffuse into the cultures. The biofilms were grown with and without the addition of 1 mM Mn(II) and the culture medium was reduced with 20 µM Na_2S. After two weeks of incubation, the biofilms were collected and analysed by XRD. Manganese oxides and carbonates phases formed in biofilms incubated with Mn(II), and elemental sulfur formed in biofilms grown without Mn(II). The formation of detectable quantities of manganese oxides in photosynthetic cultures incubated in the anaerobic glove box further demonstrated the negligible role of oxygen diffusion in the oxidation of manganese.

Acquisition of phototrophy in green sulfur bacteria

Phototrophy within stem-group green sulfur bacteria (GSB) and stem-group green non-sulfur bacteria (GNS) could have been acquired at any point before their post-GOE diversification events. Without additional information, it is not possible to infer where along these branches phototrophy was acquired, but the evolutionary history of bacteriochlorophyll biosynthesis may provide a strong clue. Phylogenies of protein families involved in bacteriochlorophyll biosynthesis have a complex evolutionary history across phototrophic lineages, including gene duplications within the stem-group GSB, and multiple horizontal gene transfer events between GSB and GNS lineages[67]. Specifically, the genes encoding BchH and BchM were transferred from within crown-group GNS to stem-group GSB, with the gene encoding BchH undergoing a duplication shortly before crown-group GSB. BchI is also observed to duplicate in the GSB stem, with one paralogue being transferred to stem GNS. These observations indicate that phototrophy must have existed in these lineages at the time of any bacteriochlorophyll-synthesis-gene duplications, or any divergence of a horizontal-gene-transfer donor lineage. A substantial history of phototrophy within the GSB stem lineage can be inferred from these events (Extended Data Fig. 6). Future molecular clock studies that include these gene tree histories may be able to constrain the time interval for phototrophy in the GSB stem; but the Bch protein histories alone suggest that phototrophy within GSB existed earlier than the appearance of the GSB or GNS crown groups.

Reporting summary

Further information on research design is available in the Nature Research Reporting Summary linked to this paper.

Data availability

Sequence data are available as FASTQ files at the National Center for Biotechnology Information (NCBI) via Sequence Read Archive (SRA), under the SRA accession number SRP133329. The datasets that support the findings of this study are available from the figshare repository (https://figshare.com/), with the identifiers 10.6084/m9.figshare.9738515, 10.6084/m9.figshare.9738725, 10.6084/m9.figshare.9738776, 10.6084/m9.figshare.9738905, 10.6084/m9.figshare.9738797, 10.6084/m9.figshare.9738878, 10.6084/m9.figshare.9738887, and 10.6084/m9.figshare.9738896. All other supporting data that support the findings of this study are available from the corresponding authors.

29. Balch, W. E. & Wolfe, R. S. New approach to the cultivation of methanogenic bacteria: 2-mercaptoethanesulfonic acid (HS-CoM)-dependent growth of *Methanobacterium ruminantium* in a pressureized atmosphere. *Appl. Environ. Microbiol.* **32**, 781–791 (1976).
30. Sim, M. S., Bosak, T. & Ono, S. Large sulfur isotope fractionation does not require disproportionation. *Science* **333**, 74–77 (2011).
31. Sim, M. S., Ono, S., Donovan, K., Templer, S. P. & Bosak, T. Effect of electron donors on the fractionation of sulfur isotopes by a marine *Desulfovibrio* sp. *Geochim. Cosmochim. Acta* **75**, 4244–4259 (2011).
32. Liang, J., Bai, Y., Men, Y. & Qu, J. Microbe–microbe interactions trigger Mn(II)-oxidizing gene expression. *ISME J.* **11**, 67–77 (2017).
33. Ljungdahl, L. & Wiegel, J. in *Manual of Industrial Microbiology and Biotechnology* (eds Demain, A. L. & Soloman, N. E.) 115–127 (American Society for Microbiology, 1986).
34. Pfennig, N. *Rhodocyclus purpureus* gen. nov. and sp. nov., a ring-shaped, vitamin B12-requiring member of the family Rhodospirillaceae. *Int. J. Syst. Evol. Microbiol.* **28**, 283–288 (1978).
35. Benson, D. A. et al. GenBank. *Nucleic Acids Res.* **41**, D36–D42 (2013).
36. Caporaso, J. G. et al. Global patterns of 16S rRNA diversity at a depth of millions of sequences per sample. *Proc. Natl Acad. Sci. USA* **108**, 4516–4522 (2011).
37. Caporaso, J. G. et al. QIIME allows analysis of high-throughput community sequencing data. *Nat. Methods* **7**, 335–336 (2010).
38. Aronesty, E. Comparison of sequencing utility programs. *Open Bioinform. J.* **7**, 1–8 (2013).
39. Edgar, R. C., Haas, B. J., Clemente, J. C., Quince, C. & Knight, R. UCHIME improves sensitivity and speed of chimera detection. *Bioinformatics* **27**, 2194–2200 (2011).
40. McDonald, D. et al. An improved Greengenes taxonomy with explicit ranks for ecological and evolutionary analyses of bacteria and archaea. *ISME J.* **6**, 610–618 (2012).
41. Price, M. N., Dehal, P. S. & Arkin, A. P. FastTree 2—approximately maximum-likelihood trees for large alignments. *PLoS ONE* **5**, e9490 (2010).
42. Segata, N. et al. Metagenomic biomarker discovery and explanation. *Genome Biol.* **12**, R60 (2011).
43. Momper, L. M., Reese, B. K., Carvalho, G., Lee, P. & Webb, E. A. A novel cohabitation between two diazotrophic cyanobacteria in the oligotrophic ocean. *ISME J.* **9**, 882–893 (2015).
44. Bolger, A. M., Lohse, M. & Usadel, B. Trimmomatic: a flexible trimmer for Illumina sequence data. *Bioinformatics* **30**, 2114–2120 (2014).
45. Li, H. et al. The Sequence Alignment/Map format and SAMtools. *Bioinformatics* **25**, 2078–2079 (2009).
46. Laczny, C. C. et al. VizBin – an application for reference-independent visualization and human-augmented binning of metagenomic data. *Microbiome* **3**, 1 (2015).
47. Parks, D. H., Imelfort, M., Skennerton, C. T., Hugenholtz, P. & Tyson, G. W. CheckM: assessing the quality of microbial genomes recovered from isolates, single cells, and metagenomes. *Genome Res.* **25**, 1043–1055 (2015).
48. Huntemann, M. et al. The standard operating procedure of the DOE-JGI Microbial Genome Annotation Pipeline (MGAP v.4). *Stand. Genomic Sci.* **10**, 86 (2015).
49. Mansor, M. & Macalady, J. L. Draft genome sequence of lampenflora *Chlorobium limicola* strain Frasassi in a sulfidic cave system. *Genome Announc.* **4**, e00357-16 (2016).
50. Ridge, J. P. et al. A multicopper oxidase is essential for manganese oxidation and laccase-like activity in *Pedomicrobium* sp. ACM 3067. *Environ. Microbiol.* **9**, 944–953 (2007).
51. Anderson, C. R. et al. Mn(II) oxidation is catalyzed by heme peroxidases in "*Aurantimonas manganoxydans*" strain SI85-9A1 and *Erythrobacter* sp. strain SD-21. *Appl. Environ. Microbiol.* **75**, 4130–4138 (2009).
52. Altschul, S. F. et al. Gapped BLAST and PSI-BLAST: a new generation of protein database search programs. *Nucleic Acids Res.* **25**, 3389–3402 (1997).
53. Nesbitt, H. & Banerjee, D. Interpretation of XPS Mn(2p) spectra of Mn oxyhydroxides and constraints on the mechanism of MnO_2 precipitation. *Am. Mineral.* **83**, 305–315 (1998).
54. Oku, M., Hirokawa, K. & Ikeda, S. X-ray photoelectron spectroscopy of manganese–oxygen systems. *J. Electron Spectrosc. Relat. Phenom.* **7**, 465–473 (1975).
55. Han, X., Zhang, J., Du, F., Cheng, J. & Chen, J. Porous calcium–manganese oxide microspheres for electrocatalytic oxygen reduction with high activity. *Chem. Sci. (Camb.)* **4**, 368–376 (2013).
56. Audi, A. A. & Sherwood, P. M. A. Valence-band X-ray photoelectron spectroscopic studies of manganese and its oxides interpreted by cluster and band structure calculations. *Surf. Interface Anal.* **33**, 274–282 (2002).
57. Toupin, M., Brousse, T. & Bélanger, D. Charge storage mechanism of MnO_2 electrode used in aqueous electrochemical capacitor. *Chem. Mater.* **16**, 3184–3190 (2004).
58. Foord, J., Jackman, R. & Allen, G. An X-ray photoelectron spectroscopic investigation of the oxidation of manganese. *Philos. Mag. A Phys. Condens. Matter Defects Mech. Prop.* **49**, 657–663 (1984).
59. Božin, E. S. et al. Structure of $CaMnO_3$ in the range $10K \leqslant T \leqslant 550$ K from neutron time-of-flight total scattering. *J. Phys. Chem. Solids* **69**, 2146–2150 (2008).
60. Cline, J. D. Spectrophotometric determination of hydrogen sulfide in natural waters. *Limnol. Oceanogr.* **14**, 454–458 (1969).
61. Krumbein, W. E. & Altman, H. J. A new method for the detection and enumeration of manganese-oxidizing and -reducing microorganisms. *Helgol. Wiss. Meeresunters.* **25**, 347–356 (1973).
62. Murray, J. W., Balistrieri, L. S. & Paul, B. The oxidation state of manganese in marine sediments and ferromanganese nodules. *Geochim. Cosmochim. Acta* **48**, 1237–1247 (1984).
63. Anschutz, P., Dedieu, K., Desmazes, K. & Chaillou, G. Speciation, oxidation state, and reactivity of particulate manganese in marine sediments. *Chem. Geol.* **218**, 265–279 (2005).
64. O'Toole, G. A. Microtiter dish biofilm formation assay. *J. Vis. Exp.* **47**, e2437 (2011).
65. Pajusalu, M., Borlina, C. S., Seager, S., Ono, S. & Bosak, T. Open-source sensor for measuring oxygen partial pressures below 100 microbars. *PLoS ONE* **13**, e0206678 (2018).

66. Lehner, P. et al. LUMOS–a sensitive and reliable optode system for measuring dissolved oxygen in the nanomolar range. *PLoS ONE* **10**, e0128125 (2015).
67. Sousa, F. L., Shavit-Grievink, L., Allen, J. F. & Martin, W. F. Chlorophyll biosynthesis gene evolution indicates photosystem gene duplication, not photosystem merger, at the origin of oxygenic photosynthesis. *Genome Biol. Evol.* **5**, 200–216 (2013).
68. Gibson, J. A. E. et al. Geochemistry of ice-covered, meromictic lake A in the Canadian High Arctic. *Aquat. Geochem.* **8**, 97–119 (2002).
69. Green, W. J., Ferdelman, T. G. & Canfield, D. E. Metal dynamics in Lake Vanda (Wright Valley, Antarctica).*Chem. Geol.* **76**, 85–94 (1989).
70. Dickman, M. & Ouellet, M. Limnology of Garrow Lake, NWT, Canada. *Polar Rec. (Gr. Brit.)* **23**, 531–549 (1987).
71. Gallagher, J. B. in *Antarctic Nutrient Cycles and Food Webs* (eds. Siegfried, W. R. et al.) 234–237 (Springer, 1985).
72. Savvichev, A. S. et al. Microbial processes of the carbon and sulfur cycles in an ice-covered, iron-rich meromictic lake Svetloe (Arkhangelsk region, Russia).*Environ. Microbiol.* **19**, 659–672 (2017).
73. Tebo, B. M. Manganese (II) oxidation in the suboxic zone of the Black Sea. *Deep-Sea Res.* **38**, S883–S905 (1991).
74. Su, J. et al. CotA, a multicopper oxidase from *Bacillus pumilus* WH4, exhibits manganese-oxidase activity. *PLoS ONE* **8**, e60573 (2013).
75. Su, J. et al. Catalytic oxidation of manganese (II) by multicopper oxidase CueO and characterization of the biogenic Mn oxide. *Water Res.* **56**, 304–313 (2014).

Acknowledgements We thank the current members of the Bosak laboratory, the Simons Foundation Collaboration on the Origins of Life (no. 327126 to T.B. and no. 339603 to G.F.), FESD NSF project (no. 1338810 to T.B.) and NSF Integrated Earth Systems (no. 1615426 to G.F. and T.B.). The NSF award number DMR-1419807 funded MIT Center for Material Science and Engineering (part of Materials Research Science and Engineering Center, NSF ECCS. award no. 1541959) funded the Harvard University Center for Nanoscale Systems (CNS), a member of the National Nanotechnology Coordinated Infrastructure Network (NNCI). The DOE Office of Science User Facility under contract no. DE-AC02-05CH11231 supports the Advanced Light Source and BI L12.3.2. M.P. and T.B. received funding from the John Templeton foundation, and M.P. was also supported by the Professor Amar G. Bose Research Grant Program (MIT).

Author contributions M.D. and T.B. conceived and designed the project. M.D. performed microbial enrichment experiments and analysed data. M.D. and N.T. performed synchrotron μXRD diffraction and analysed data. M.D. and M.P. performed oxygen concentration measurement experiments and analysed data. V.K.-C. and S.R. analysed the composition of microbial communities and performed bioinformatics analyses. V.K.-C. and A.F.-S. conducted bioinformatics analyses of the co-cultures and pure culture genomes. G.F. wrote about the molecular evolution of photosynthetic groups and contributed Extended Data Fig. 6. N.B. contributed to the writing by commenting on Archaean geology. M.D. and T.B. wrote the manuscript with input from M.P. and V.K.-C., N.B. and G.F. All co-authors reviewed and approved the final manuscript.

Competing interests The authors declare no competing interests.

Additional information
Supplementary information is available for this paper at https://doi.org/10.1038/s41586-019-1804-0.
Correspondence and requests for materials should be addressed to M.D. or T.B.
Reprints and permissions information is available at http://www.nature.com/reprints.

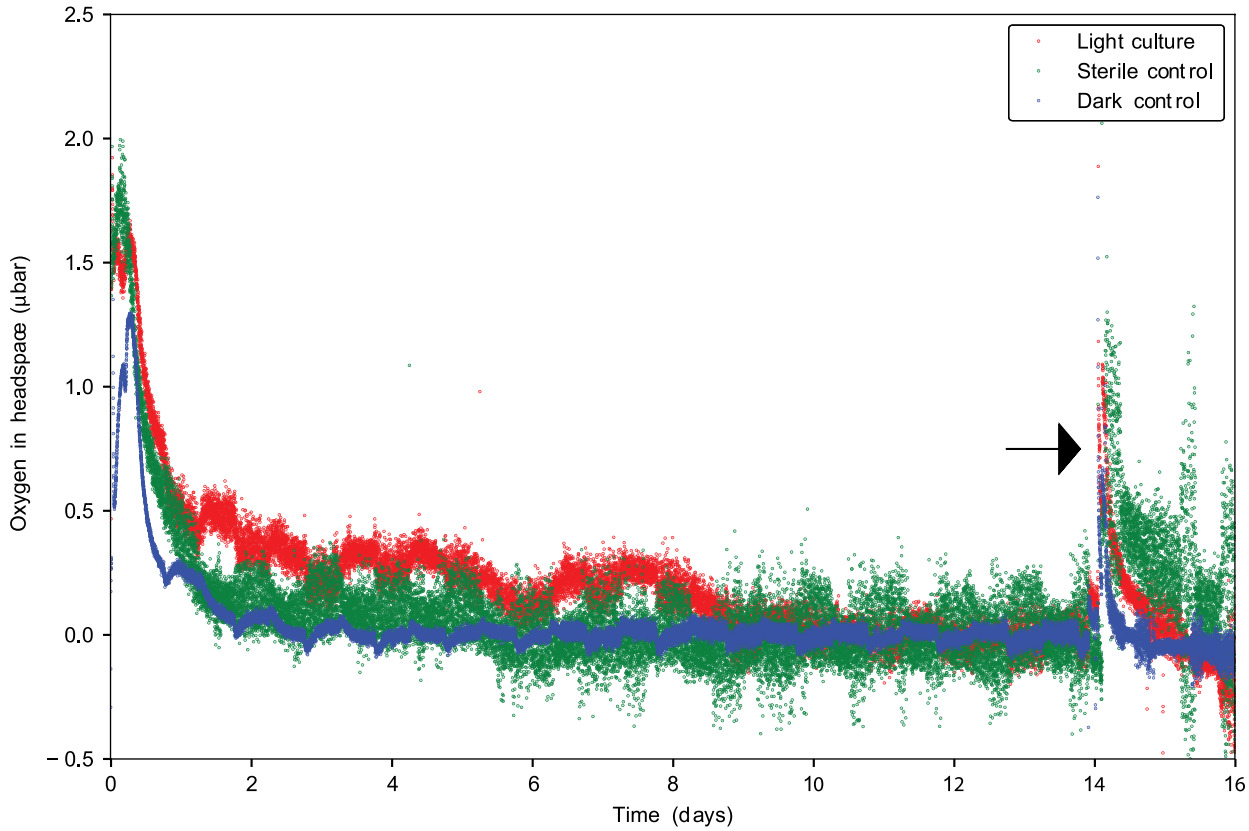

Extended Data Fig. 1 | Partial pressure of oxygen in the headspace of enrichment cultures and dark controls. Oxygen concentration (µatm) measured in the headspaces of 150-ml serum bottles that contained 100 ml of MFGL medium, 50 µM sulfide and 1 mM $MnCl_2$. One inoculated culture was incubated in the light (red points) and another in the dark (blue points). The sterile control (green points) was incubated in the light. Individual points are measurements by the oxygen sensor taken every 48.2 s. To control for sensor drift and recalibrate the zero point of the sensor, the bottles were flushed with oxygen-free N_2 on day 14 (black arrow) after the inoculation. The fluorescence reading value after the stabilization was set as zero. The diurnal oscillations in O_2 concentration reflect temperature changes induced by the proximity to the light bulb with a 12:12 h day:night cycle. Oxygen concentrations in all cultures were lower than 1 nM at all times after about 12 h and before the flushing on day 14. All data are representative of two independent measurements.

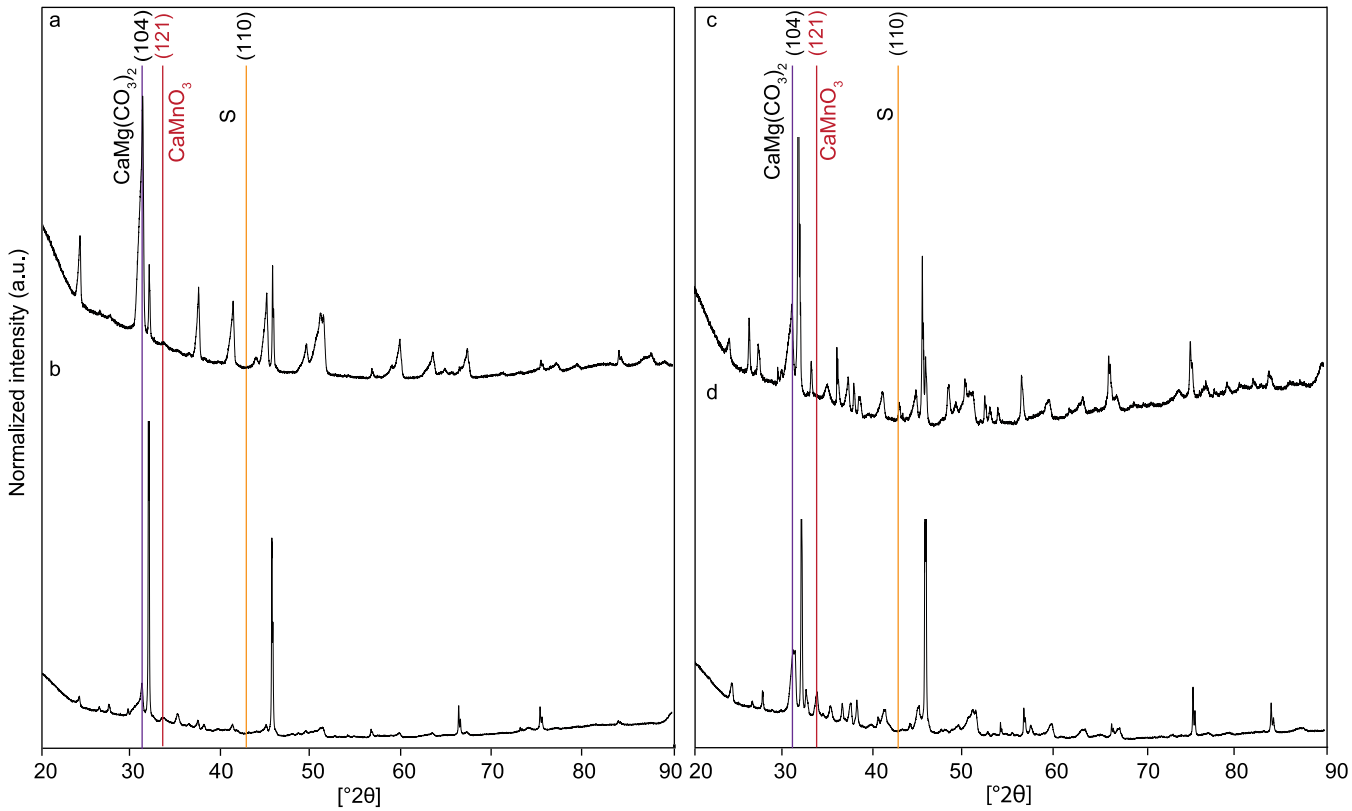

Extended Data Fig. 2 | XRD spectra of biofilm samples incubated in the light for two weeks. a–d, These biofilms were not treated to remove manganese oxides before inoculation. **a**, One millimolar Mn(II) and 0.05 mM Na_2S. **b**, Mn(II) at 0.1 mM, and 0.05 mM Na_2S. **c**, One millimolar Mn(II) and 1 mM Na_2S. **d**, One millimolar Mn(II) and 0.25 mM Na_2S. Purple line shows the highest intensity peak at 2θ of 30.870° for the basal reflection of (104) plane of dolomite, $CaMg(CO_3)_2$. Red line shows the highest intensity peak at 2θ of 33.867° for the basal reflection of (121) plane of $CaMnO_3$. Orange line shows the highest intensity peak at 2θ of 42.845° for the basal reflection of (110) plane of S^0. All data are representative of three independent measurements.

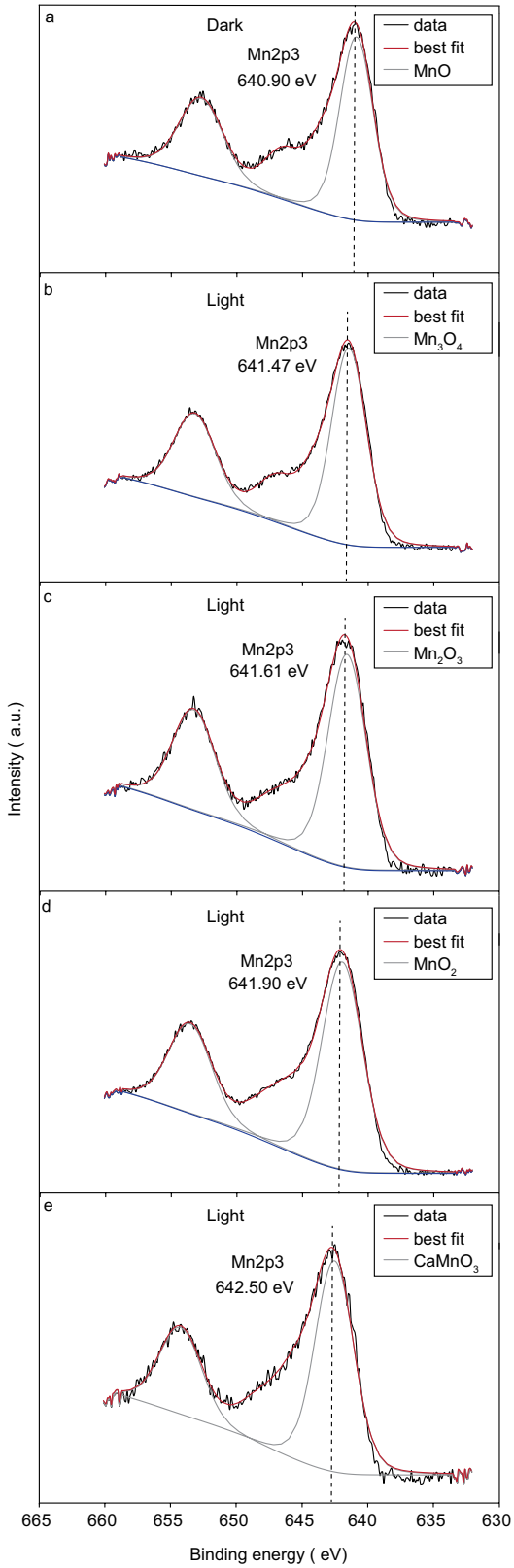

Extended Data Fig. 3 | XPS of the 2*p* spectral region of manganese in two-week-old microbial cultures. a, Biofilm incubated in the dark. The Mn2$p_{3/2}$ main peak of the sample fits the MnO standard at binding energy of 640.90 eV that corresponds to the redox state of Mn(II). **b**, Biofilm incubated in the light. The Mn2$p_{3/2}$ main peak of the sample fits the Mn_3O_4 standard at binding energy of 641.47 eV that corresponds to Mn(III) and Mn(II). **c**, Biofilm incubated in the light (a different region to that shown in **b** and **d**). The Mn2$p_{3/2}$ main peak of the sample fits the Mn_2O_3 standard at binding energy of 641.61 eV that corresponds to Mn(III). **d**, Biofilm incubated in the light (a different region to that shown in **b**, **c**). The Mn2$p_{3/2}$ main peak of the sample fits MnO_2 standard at binding energy of 641.90 eV that corresponds to redox state of Mn(IV). **e**, Biofilm incubated in the light (a different region to that shown in **c**, **d**). The Mn2$p_{3/2}$ main peak of the sample fits the $CaMnO_3$ standard at binding energy of 642.50 eV that corresponds to Mn(IV). All data are representative of three independent measurements.

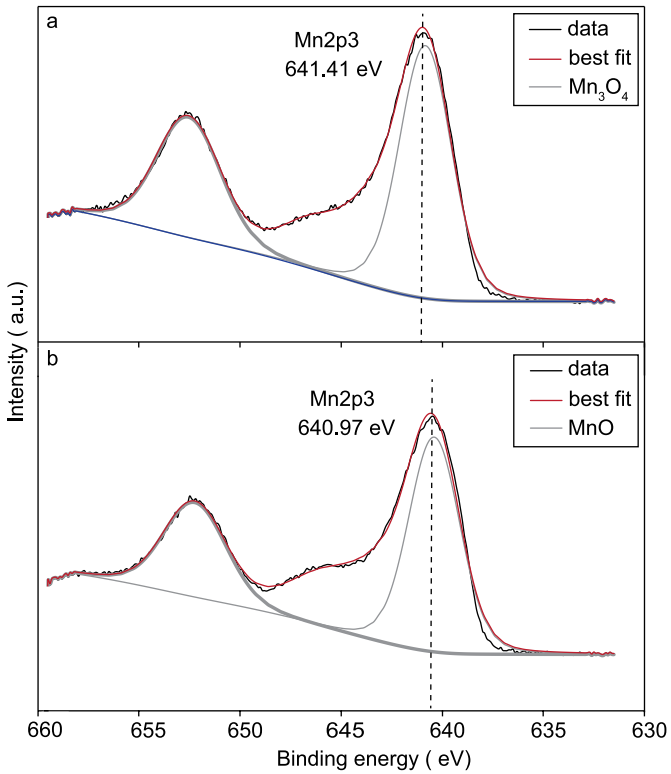

Extended Data Fig. 4 | Test of manganese-oxidizing activity in cell suspensions of photosynthetic cultures enriched under two conditions. Results of XPS analysis of the 2*p* spectral region of manganese are shown. **a**, Culture enriched on 1 mM Mn(II) and 0.05 mM H_2S (condition (1)). The Mn2$p_{3/2}$ main peak of the sample fits Mn_3O_4 standard at binding energy of 641.41 eV. This corresponds to Mn(II) and Mn(III). **b**, Culture enriched on 1 mM H_2S (condition (2)). The Mn2$p_{3/2}$ main peak of the sample fits MnO standard at binding energy of 640.97 eV and corresponds to the redox state Mn(II). A detailed experimental protocol is described in 'Interpretation of XPS spectra' in the Methods, and summarized in Extended Data Table 3. All data are representative of three independent measurements.

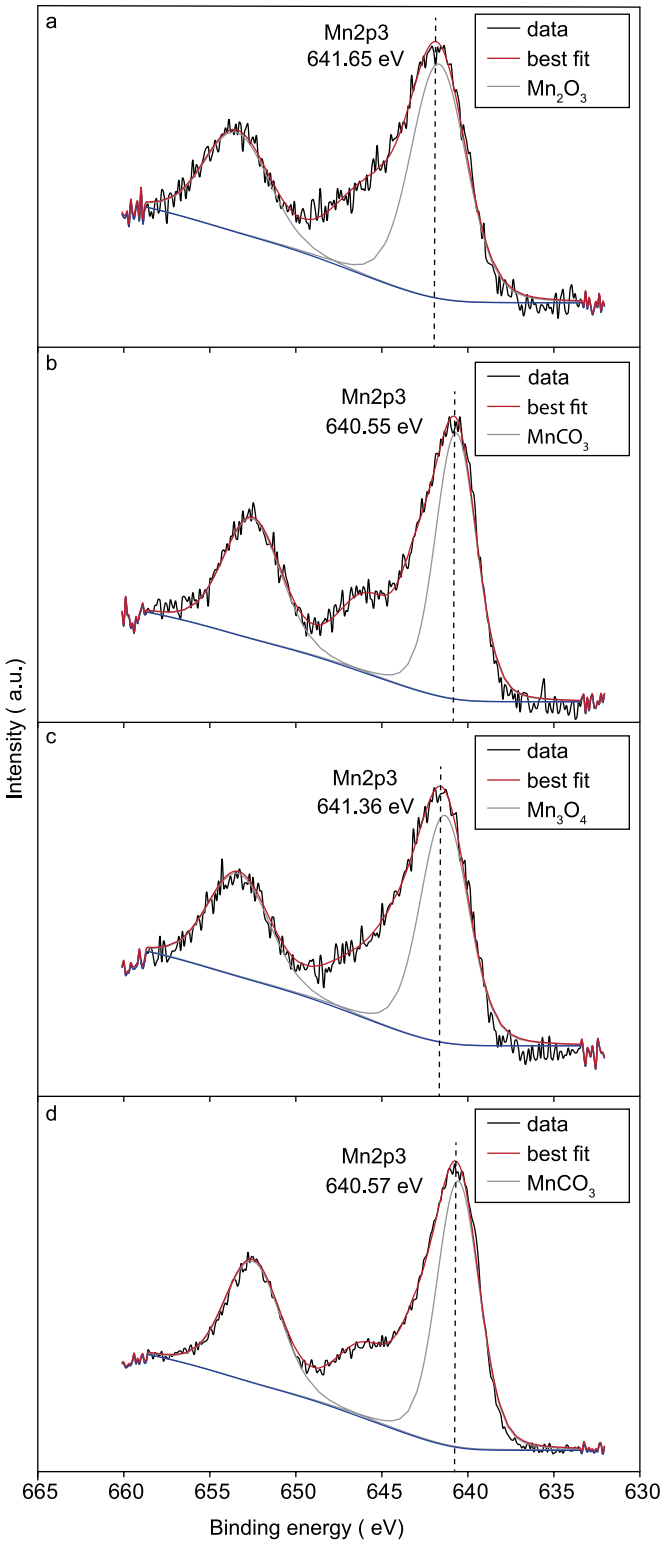

Extended Data Fig. 5 | Test of manganese-oxidizing activity in cell suspensions of pure cultures and co-cultures of *C. limicola*, *C. tepidum* and *G. lovleyi*. **a**–**d**, Results of XPS analysis of the 2*p* spectral region of manganese are shown. **a**, *C. limicola*, *C. tepidum and G. lovleyi*. The Mn2$p_{3/2}$ main peak of the sample fits Mn_2O_3 standard at binding energy of 641.65 eV. This corresponds to a valence state of Mn(III). **b**, *C. limicola* and *C. tepidum*. The Mn2$p_{3/2}$ main peak of the sample fits $MnCO_3$ standard at binding energy of 640.55 eV and corresponds to the redox state Mn(II). **c**, *C. limicola* and *G. lovleyi*. The Mn2$p_{3/2}$ main peak of the sample fits Mn_3O_4 standard at binding energy of 641.36eV. **d**, *C. tepidum* and *G. lovleyi*. The Mn2$p_{3/2}$ main peak of the sample fits $MnCO_3$ standard at binding energy of 640.57 eV. A detailed experimental protocol is described in 'Probing the redox state of manganese in co-cultures' in the Methods. All co-cultures were grown with 1 mM Mn(II) and 0.05 mM H_2S for 2 weeks in the light. All data are representative of three independent measurements.

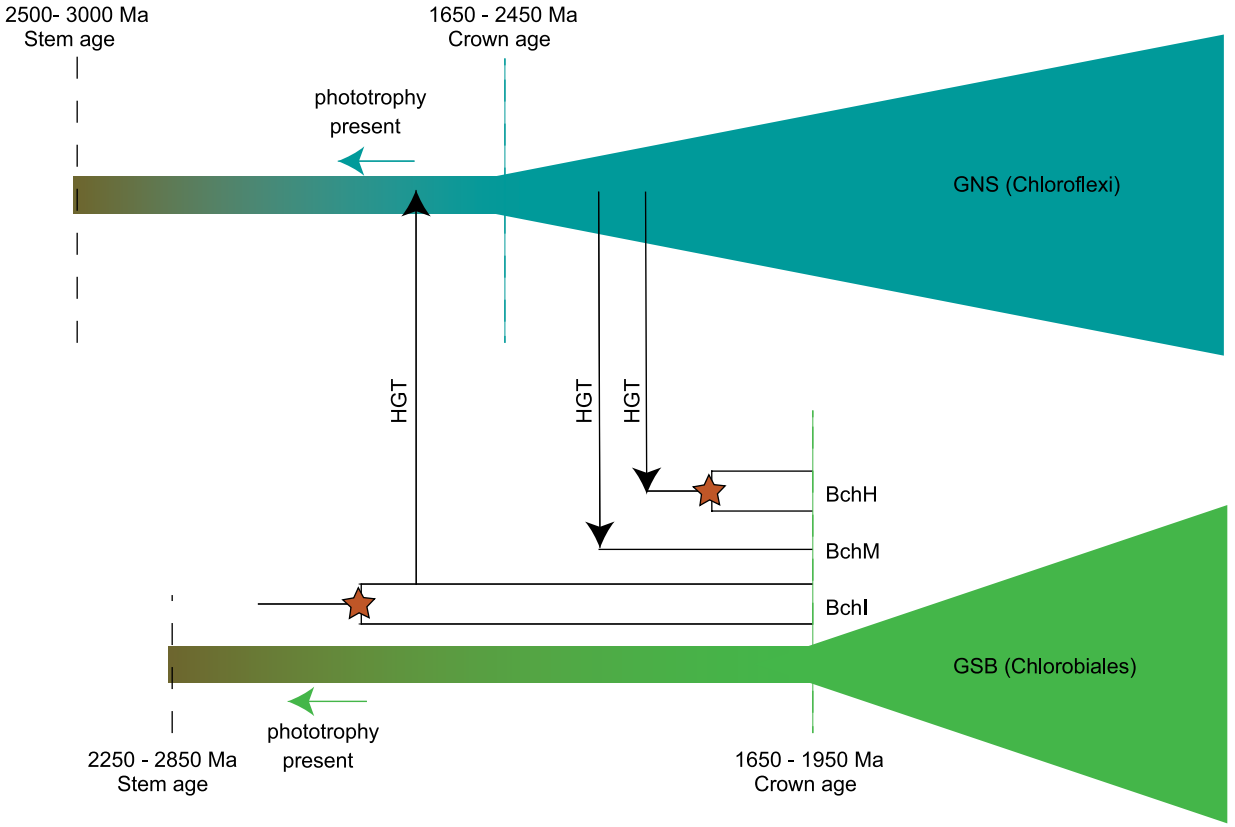

Extended Data Fig. 6 | Reticulate history of bacteriochlorophyll-biosynthesis genes supports a long history of phototrophy in the Chlorobiales stem lineage. Horizontal gene transfers and gene duplications of bacteriochlorophyll genes were taken from a previous publication[67]. Age estimates for crown Chlorobi and GNS groups were taken from a previous publication[26].

Extended Data Table 1 | Aquatic environments with H_2S and manganese in the photic zone

Water body	H_2S (μM)	Mn(II) (μM)	Photic Zone	Reference
Lake A	230	140	Green Sulfur Bacteria	68
Lake Vanda	240	120	Unclear	69
Garrow Lake	20	18	Green Sulfur Bacteria	70
Sombre Lake	1.2	68	Green Sulfur Bacteria	71
Svetloe Lake	2	60	Green Sulfur Bacteria	72
Black Sea	2	8.4	Green Sulfur Bacteria	73
Green Lake	20-30	50-60	Green Sulfur Bacteria	8

Data are from previous publications[8,68–73].

Extended Data Table 2 | Shake tube and transfer procedures used to obtain enrichments from conditions 1 and 2

First round shake tube	Incubation period, (days)	Colonies	Transfer into liquid medium	Incubation period (days)	Growth[1]	Enrichment	
20 μM Na_2S, 1 mM $MnCl_2$	30	Black and dark brown	Brown colony; 0.02 mM Na_2S, 1 mM $MnCl_2$	30	+	Condition 1	
1 mM Na_2S	30	Black, white and dark brown	Brown colony; 1 mM Na_2S	30	+++	Condition 2	
Second round shake tube	**Incubation period (days)**	**Colonies**	**Transfer into liquid medium**	**Incubation period (days)**	**Growth[1]**	**Enrichment**	**Microbes present in enrichment culture[2]**
0.02 mM Na_2S, 1 mM $MnCl_2$	30	Brown, dark brown	Brown colony; 0.02 mM Na_2S, 1 mM $MnCl_2$	30	+	Condition 1	*Chlorobium limicola, Geobacter lovleyi*, others[3]
1 mM Na_2S	30	Brown, dark brown	Brown colony; 1 mM Na_2S	30	+++	Condition 2	*Chlorobium limicola, Desulfomicrobium sp.*

[1]Growth of colonies transferred from shake to a liquid medium of the same chemical composition. +, low microbial growth; +++, high microbial growth.

[2]Microbial composition determined by metagenomic sequencing.

[3]*A. equifetale, Alistipes* sp. HGB5, and *C. oshimai*.

Extended Data Table 3 | Summary of the methods used to examine the redox state of manganese in enrichment cultures

Enrichment condition	Transfer condition	Transfer MFGL medium composition	Incubation time (days)	Growth[1]	Mn oxidation activity[2]
Condition 1	Cell suspension	0.02 mM Na_2S, 1mM $MnCl_2$	3	-	+
Condition 2	Cell suspension	0.02 mM Na_2S, 1 mM $MnCl_2$	3	-	-
Condition 1	5 % inoculum	0.02 mM Na_2S, 1mM $MnCl_2$	7	-	-
Condition 2	5 % inoculum	0.02 mM Na_2S, 1mM $MnCl_2$	7	+	-

[1]+ or – indicates visible growth (+) of the co-culture, or not (–)

[2]Manganese oxidation in the enrichment cultures was examined using XPS; + or –, presence (+) or absence (–) of Mn(II)-oxidizing activity in the microbial co-culture.

Extended Data Table 4 | Mn(II)-oxidation genes with confirmed function compared using BLASTp v. 2.6.0+ against the genome of *C. limicola* SR-12

Locus ID	Gene Annotation	Gene Name	Organism	Ref.	% identity	e. value	bit score
PputGB1_3353	animal heme peroxidase	*mopA*	*Pseudomonas putida*	[18]	46	1.0E-08	57.4
WP_007817484	animal heme peroxidase	*ahpL*	*Roseobacter* sp. AzwK-3b	[19]	40	*7.0E-06*	48.5
WP_009209951	animal heme peroxidase	*mopA*	*Aurantimonas manganoxydans*	[51]	47	*1.0E-07*	53.5
WP_006837219	multi-copper oxidase	*mnxG*	*Bacillus* sp. strain SG-1	[17]	no hits		
WP_076798083	multi-copper oxidase / billirubin oxidase	*boxA*	*Arthrobacter* sp. QXT-31	[32]	no hits		
AFL56752	multi-copper oxidase, type 2	*cotA*	*Bacillus pumilus* WH4	[74]	no hits		
CAJ19378	multi-copper oxidase	*moxA*	*Pedomicrobium* sp. ACM 3067	[50]	no hits		
NP_745328	multi-copper oxidase / billirubin oxidase	*mcoA*	*Pseudomonas putida*	[18]	no hits		
EG12318	multi-copper oxidase	*cueO*	*Escherichia coli*	[75]	no hits		

All animal haem peroxidases also hit the haemolysin-type calcium-binding region in *C. limicola* ($e = 3 \times 10^{-21}$, bit score = 98.6). Data are from previous publications[17–19,32,50,51,74,75].

nature research

Corresponding author(s): M. Daye et al., 2018-06-07850D

Double-blind peer review submissions: write DBPR and your manuscript number here instead of author names.

☐ Initial submission ☐ Revised version ☑ Final submission

Reporting Summary

Nature Research wishes to improve the reproducibility of the work that we publish. This form provides structure for consistency and transparency in reporting. For further information on Nature Research policies, see Authors & Referees and the Editorial Policy Checklist.

Please do not complete any field with "not applicable" or n/a. Refer to the help text for what text to use if an item is not relevant to your study.
For final submission: please carefully check your responses for accuracy; you will not be able to make changes later.

Statistical parameters

When statistical analyses are reported, confirm that the following items are present in the relevant location (e.g. figure legend, table legend, main text, or Methods section).

n/a	Confirmed	
☑	☐	The exact sample size (*n*) for each experimental group/condition, given as a discrete number and unit of measurement
☑	☐	An indication of whether measurements were taken from distinct samples or whether the same sample was measured repeatedly
☑	☐	The statistical test(s) used AND whether they are one- or two-sided *Only common tests should be described solely by name; describe more complex techniques in the Methods section.*
☑	☐	A description of all covariates tested
☑	☐	A description of any assumptions or corrections, such as tests of normality and adjustment for multiple comparisons
☑	☐	A full description of the statistics including central tendency (e.g. means) or other basic estimates (e.g. regression coefficient) AND variation (e.g. standard deviation) or associated estimates of uncertainty (e.g. confidence intervals)
☐	☑	For null hypothesis testing, the test statistic (e.g. *F*, *t*, *r*) with confidence intervals, effect sizes, degrees of freedom and *P* value noted *Give P values as exact values whenever suitable.*
☑	☐	For Bayesian analysis, information on the choice of priors and Markov chain Monte Carlo settings
☑	☐	For hierarchical and complex designs, identification of the appropriate level for tests and full reporting of outcomes
☑	☐	Estimates of effect sizes (e.g. Cohen's *d*, Pearson's *r*), indicating how they were calculated
☐	☑	Clearly defined error bars *State explicitly what error bars represent (e.g. SD, SE, CI)*

Our web collection on statistics for biologists may be useful.

Software and code

Policy information about availability of computer code

Data collection: No software has been used to collect data.

Provide a description of all commercial, open source and custom code used to collect the data in this study, specifying the version used OR state that no software was used.

Data analysis: Microsoft excel has been used to analyze, plot and perform statistical analyses of the data.

Provide a description of all commercial, open source and custom code used to analyse the data in this study, specifying the version used OR state that no software was used.

For manuscripts utilizing custom algorithms or software that are central to the research but not yet described in published literature, software must be made available to editors/reviewers upon request. We strongly encourage code deposition in a community repository (e.g. GitHub). See the Nature Research guidelines for submitting code & software for further information.

Data

Policy information about availability of data

All manuscripts must include a data availability statement. This statement should provide the following information, where applicable:

- Accession codes, unique identifiers, or web links for publicly available datasets
- A list of figures that have associated raw data
- A description of any restrictions on data availability

Data is deposited on Figshare and made availble through weblinks.
The data will be published on figshare and will be made available for public through Digital Object Identifier (DOI) weblinks after publication of the manuscript.

We encourage data deposition in Dryad or Figshare.

Field-specific reporting

Please select the best fit for your research. If you are not sure, read the appropriate sections before making your selection.

☑ Life sciences ☐ Behavioural & social sciences ☐ Ecological, evolutionary & environmental sciences

Life sciences study design

All studies must disclose on these points even when the disclosure is negative.

Sample size	No sample size (s) calculation was performed. For each experiment we do test for diffrent chemical conditions and for each variable we have triplicates (n=3). Each experiment can have at least 4 different variables (v=3) which is equivalent: s=n*v=12
Data exclusions	No data exclusion performed in this study
Replication	For each analysis, triplicates were performed. Each experiment was at least 3 times repeated to ensure reproductibility. Each experimet was repeated independently two -five times to ensure similar results.
Randomization	This is not relevant to the study. We are examining one type of microbial biofilm.
Blinding	Not relevant to the study since we are studying the manganese anaerobic oxidation in one type of photosynthetic microbial biofilm.

Behavioural & social sciences study design

All studies must disclose on these points even when the disclosure is negative.

Study description	*Briefly describe the study type including whether data are quantitative, qualitative, or mixed-methods (e.g. qualitative cross-sectional, quantitative experimental, mixed-methods case study).*
Research sample	*State the research sample (e.g. Harvard university undergraduates, villagers in rural India) and provide relevant demographic information (e.g. age, sex) and indicate whether the sample is representative. Provide a rationale for the study sample chosen. For studies involving existing datasets, please describe the dataset and source.*
Sampling strategy	*Describe the sampling procedure (e.g. random, snowball, stratified, convenience). Describe the statistical methods that were used to predetermine sample size OR if no sample-size calculation was performed, describe how sample sizes were chosen and provide a rationale for why these sample sizes are sufficient. For qualitative data, please indicate whether data saturation was considered, and what criteria were used to decide that no further sampling was needed.*
Data collection	*Provide details about the data collection procedure, including the instruments or devices used to record the data (e.g. pen and paper, computer, eye tracker, video or audio equipment) whether anyone was present besides the participant(s) and the researcher, and whether the researcher was blind to experimental condition and/or the study hypothesis during data collection.*
Timing	*Indicate the start and stop dates of data collection. If there is a gap between collection periods, state the dates for each sample cohort.*
Data exclusions	*If no data were excluded from the analyses, state so OR if data were excluded, provide the exact number of exclusions and the rationale behind them, indicating whether exclusion criteria were pre-established.*
Non-participation	*State how many participants dropped out/declined participation and the reason(s) given OR provide response rate OR state that no participants dropped out/declined participation.*
Randomization	*If participants were not allocated into experimental groups, state so OR describe how participants were allocated to groups, and if allocation was not random, describe how covariates were controlled.*

Ecological, evolutionary & environmental sciences study design

All studies must disclose on these points even when the disclosure is negative.

Study description	*Briefly describe the study. For quantitative data include treatment factors and interactions, design structure (e.g. factorial, nested, hierarchical), nature and number of experimental units and replicates.*

Research sample	*Describe the research sample (e.g. a group of tagged Passer domesticus, all Stenocereus thurberi within Organ Pipe Cactus National Monument), and provide a rationale for the sample choice. When relevant, describe the organism taxa, source, sex, age range and any manipulations. State what population the sample is meant to represent when applicable. For studies involving existing datasets, describe the data and its source.*
Sampling strategy	*Note the sampling procedure. Describe the statistical methods that were used to predetermine sample size OR if no sample-size calculation was performed, describe how sample sizes were chosen and provide a rationale for why these sample sizes are sufficient.*
Data collection	*Describe the data collection procedure, including who recorded the data and how.*
Timing and spatial scale	*Indicate the start and stop dates of data collection, noting the frequency and periodicity of sampling and providing a rationale for these choices. If there is a gap between collection periods, state the dates for each sample cohort. Specify the spatial scale from which the data are taken*
Data exclusions	*If no data were excluded from the analyses, state so OR if data were excluded, describe the exclusions and the rationale behind them, indicating whether exclusion criteria were pre-established.*
Reproducibility	*Describe the measures taken to verify the reproducibility of experimental findings. For each experiment, note whether any attempts to repeat the experiment failed OR state that all attempts to repeat the experiment were successful.*
Randomization	*Describe how samples/organisms/participants were allocated into groups. If allocation was not random, describe how covariates were controlled. If this is not relevant to your study, explain why.*
Blinding	*Describe the extent of blinding used during data acquisition and analysis. If blinding was not possible, describe why OR explain why blinding was not relevant to your study.*

Did the study involve field work? ☐ Yes ☐ No

Field work, collection and transport

Field conditions	*Describe the study conditions for field work, providing relevant parameters (e.g. temperature, rainfall).*
Location	*State the location of the sampling or experiment, providing relevant parameters (e.g. latitude and longitude, elevation, water depth).*
Access and import/export	*Describe the efforts you have made to access habitats and to collect and import/export your samples in a responsible manner and in compliance with local, national and international laws, noting any permits that were obtained (give the name of the issuing authority, the date of issue, and any identifying information).*
Disturbance	*Describe any disturbance caused by the study and how it was minimized.*

Reporting for specific materials, systems and methods

We require information from authors about some types of materials, experimental systems and methods used in many studies. Here, indicate whether each material, system or method listed is relevant to your study. If you are not sure if a list item applies to your research, read the appropriate section before selecting a response.

Materials & experimental systems

n/a	Involved in the study
☑	☐ Unique biological materials
☑	☐ Antibodies
☑	☐ Eukaryotic cell lines
☑	☐ Palaeontology
☑	☐ Animals and other organisms
☑	☐ Human research participants

Methods

n/a	Involved in the study
☑	☐ ChIP-seq
☑	☐ Flow cytometry
☑	☐ MRI-based neuroimaging

Unique biological materials

Policy information about availability of materials

Obtaining unique materials	*Describe any restrictions on the availability of unique materials OR confirm that all unique materials used are readily available from the authors or from standard commercial sources (and specify these sources).*

Antibodies

Antibodies used	*Describe all antibodies used in the study; as applicable, provide supplier name, catalog number, clone name, and lot number.*

Validation

Describe the validation of each primary antibody for the species and application, noting any validation statements on the manufacturer's website, relevant citations, antibody profiles in online databases, or data provided in the manuscript.

Eukaryotic cell lines

Policy information about cell lines

Cell line source(s)

State the source of each cell line used.

Authentication

Describe the authentication procedures for each cell line used OR declare that none of the cell lines used were authenticated.

Mycoplasma contamination

Confirm that all cell lines tested negative for mycoplasma contamination OR describe the results of the testing for mycoplasma contamination OR declare that the cell lines were not tested for mycoplasma contamination.

Commonly misidentified lines
(See ICLAC register)

Name any commonly misidentified cell lines used in the study and provide a rationale for their use.

Palaeontology

Specimen provenance

Provide provenance information for specimens and describe permits that were obtained for the work (including the name of the issuing authority, the date of issue, and any identifying information).

Specimen deposition

Indicate where the specimens have been deposited to permit free access by other researchers.

Dating methods

If new dates are provided, describe how they were obtained (e.g. collection, storage, sample pretreatment and measurement), where they were obtained (i.e. lab name), the calibration program and the protocol for quality assurance OR state that no new dates are provided.

☐ Tick this box to confirm that the raw and calibrated dates are available in the paper or in Supplementary Information.

Animals and other organisms

Policy information about studies involving animals; ARRIVE guidelines recommended for reporting animal research

Laboratory animals

For laboratory animals, report species, strain, sex and age OR state that the study did not involve laboratory animals.

Wild animals

Provide details on animals observed in or captured in the field; report species, sex and age where possible. Describe how animals were caught and transported and what happened to captive animals after the study (if killed, explain why and describe method; if released, say where and when) OR state that the study did not involve wild animals.

Field-collected samples

For laboratory work with field-collected samples, describe all relevant parameters such as housing, maintenance, temperature, photoperiod and end-of-experiment protocol OR state that the study did not involve samples collected from the field.

Human research participants

Policy information about studies involving human research participants

Population characteristics

Describe the covariate-relevant population characteristics of the human research participants (e.g. age, gender, genotypic information, past and current diagnosis and treatment categories). If you filled out the behavioural & social sciences study design questions and have nothing to add here, write "See above."

Recruitment

Describe how participants were recruited. Outline any potential self-selection bias or other biases that may be present and how these are likely to impact results.

ChIP-seq

Data deposition

☐ Confirm that both raw and final processed data have been deposited in a public database such as GEO.

☐ Confirm that you have deposited or provided access to graph files (e.g. BED files) for the called peaks.

Data access links
May remain private before publication.

For "Initial submission" or "Revised version" documents, provide reviewer access links. For your "Final submission" document, provide a link to the deposited data.

Files in database submission

Provide a list of all files available in the database submission.

Genome browser session
(e.g. UCSC)

Provide a link to an anonymized genome browser session for "Initial submission" and "Revised version" documents only, to enable peer review. Write "no longer applicable" for "Final submission" documents.

Methodology

Replicates	*Describe the experimental replicates, specifying number, type and replicate agreement.*
Sequencing depth	*Describe the sequencing depth for each experiment, providing the total number of reads, uniquely mapped reads, length of reads and whether they were paired- or single-end.*
Antibodies	*Describe the antibodies used for the ChIP-seq experiments; as applicable, provide supplier name, catalog number, clone name, and lot number.*
Peak calling parameters	*Specify the command line program and parameters used for read mapping and peak calling, including the ChIP, control and index files used.*
Data quality	*Describe the methods used to ensure data quality in full detail, including how many peaks are at FDR 5% and above 5-fold enrichment.*
Software	*Describe the software used to collect and analyze the ChIP-seq data. For custom code that has been deposited into a community repository, provide accession details.*

Flow Cytometry

Plots

Confirm that:

☐ The axis labels state the marker and fluorochrome used (e.g. CD4-FITC).

☐ The axis scales are clearly visible. Include numbers along axes only for bottom left plot of group (a 'group' is an analysis of identical markers).

☐ All plots are contour plots with outliers or pseudocolor plots.

☐ A numerical value for number of cells or percentage (with statistics) is provided.

Methodology

Sample preparation	*Describe the sample preparation, detailing the biological source of the cells and any tissue processing steps used.*
Instrument	*Identify the instrument used for data collection, specifying make and model number.*
Software	*Describe the software used to collect and analyze the flow cytometry data. For custom code that has been deposited into a community repository, provide accession details.*
Cell population abundance	*Describe the abundance of the relevant cell populations within post-sort fractions, providing details on the purity of the samples and how it was determined.*
Gating strategy	*Describe the gating strategy used for all relevant experiments, specifying the preliminary FSC/SSC gates of the starting cell population, indicating where boundaries between "positive" and "negative" staining cell populations are defined.*

☐ Tick this box to confirm that a figure exemplifying the gating strategy is provided in the Supplementary Information.

Magnetic resonance imaging

Experimental design

Design type	*Indicate task or resting state; event-related or block design.*
Design specifications	*Specify the number of blocks, trials or experimental units per session and/or subject, and specify the length of each trial or block (if trials are blocked) and interval between trials.*
Behavioral performance measures	*State number and/or type of variables recorded (e.g. correct button press, response time) and what statistics were used to establish that the subjects were performing the task as expected (e.g. mean, range, and/or standard deviation across subjects).*

Acquisition

Imaging type(s)	*Specify: functional, structural, diffusion, perfusion.*
Field strength	*Specify in Tesla*
Sequence & imaging parameters	*Specify the pulse sequence type (gradient echo, spin echo, etc.), imaging type (EPI, spiral, etc.), field of view, matrix size, slice thickness, orientation and TE/TR/flip angle.*
Area of acquisition	*State whether a whole brain scan was used OR define the area of acquisition, describing how the region was determined.*

Diffusion MRI ☐ Used ☐ Not used

Preprocessing

Preprocessing software — *Provide detail on software version and revision number and on specific parameters (model/functions, brain extraction, segmentation, smoothing kernel size, etc.).*

Normalization — *If data were normalized/standardized, describe the approach(es): specify linear or non-linear and define image types used for transformation OR indicate that data were not normalized and explain rationale for lack of normalization.*

Normalization template — *Describe the template used for normalization/transformation, specifying subject space or group standardized space (e.g. original Talairach, MNI305, ICBM152) OR indicate that the data were not normalized.*

Noise and artifact removal — *Describe your procedure(s) for artifact and structured noise removal, specifying motion parameters, tissue signals and physiological signals (heart rate, respiration).*

Volume censoring — *Define your software and/or method and criteria for volume censoring, and state the extent of such censoring.*

Statistical modeling & inference

Model type and settings — *Specify type (mass univariate, multivariate, RSA, predictive, etc.) and describe essential details of the model at the first and second levels (e.g. fixed, random or mixed effects; drift or auto-correlation).*

Effect(s) tested — *Define precise effect in terms of the task or stimulus conditions instead of psychological concepts and indicate whether ANOVA or factorial designs were used.*

Specify type of analysis: ☐ Whole brain ☐ ROI-based ☐ Both

Statistic type for inference (See Eklund et al. 2016) — *Specify voxel-wise or cluster-wise and report all relevant parameters for cluster-wise methods.*

Correction — *Describe the type of correction and how it is obtained for multiple comparisons (e.g. FWE, FDR, permutation or Monte Carlo).*

Models & analysis

n/a	Involved in the study
☐	☐ Functional and/or effective connectivity
☐	☐ Graph analysis
☐	☐ Multivariate modeling or predictive analysis

Functional and/or effective connectivity — *Report the measures of dependence used and the model details (e.g. Pearson correlation, partial correlation, mutual information).*

Graph analysis — *Report the dependent variable and connectivity measure, specifying weighted graph or binarized graph, subject- or group-level, and the global and/or node summaries used (e.g. clustering coefficient, efficiency, etc.).*

Multivariate modeling and predictive analysis — *Specify independent variables, features extraction and dimension reduction, model, training and evaluation metrics.*